A CYLINDRICAL SHELL WITH A STRESS-FREE END WHICH CONTAINS AN AXIAL PART-THROUGH OR THROUGH CRACK

by

F. Erdogan and O.S. Yahsi

December 1983

Lehigh University

Bethlehem, Pennsylvania

THE NATIONAL AERONAUTICS AND SPACE ADMINISTRATION

GRANT NGR 39 007 011

A CYLINDRICAL SHELL WITH A STRESS-FREE END WHICH CONTAINS AN AXIAL PART-THROUGH OR THROUGH CRACK

by

F. Erdogan and O.S. Yahsi

Lehigh University, Bethlehem, PA

ABSTRACT

In this paper the interaction problem of a through or a part-through crack with a stress-free boundary in a semi-infinite cylindrical shell is considered. It is assumed that the crack lies in a meridional plane which is a plane of symmetry with respect to the external loads as well as the geometry. The circular boundary of the semi-infinite cylinder is assumed to be stress-free. By using a transverse shear theory the problem is formulated in terms of a system of singular integral equations. The line spring model is used to treat the part-through crack problem. In the case of a through crack the interaction between the perturbed stress fields due to the crack and the free boundary is quite strong and there is a considerable increase in the stress intensity factors caused by the interaction. On the other hand in the problem of a surface crack the interaction appears to be much weaker and consequently the magnification in the stress intensity factors is much less significant.

1. Introduction

The main objective of this paper is to study the effect of a stress-free boundary on the stress intensity factors in a cylindrical shell which contains a part-through or a through crack near the boundary. From the corresponding elasticity solutions of flat plates it is known that when the stress field perturbed by a crack interacts with a free boundary there is a certain magnification in the related stress intensity factors, implying that there would be a reduction in the resistance of the structure to fatigue crack propagation and fracture [1,2]. Experimental as well as analytical results also show that generally the stress intensity factors at that crack tip which is nearer to the free boundary

are greater than those at the other tip and consequently the crack would tend to propagate toward (and eventually perpendicular to) the free boundary [1-3]. This means that of the simple crack geometries in plates and shells the one which may be of the most practical interest would be the crack perpendicular to the free boundary.

In shells additional magnification in the stress intensity factors is known to arise because of curvature [4-6]. In this paper the combined effect of the stress-free boundary and curvature in a cylindrical shell is studied. It is assumed the plane of the free boundary is perpendicular to the axis of the cylinder and the crack is in a meridional plane. Further, the external loads applied to the curved surfaces and the end of the cylinder are assumed to be such that the shear stresses σ_{12} and σ_{13} vanish throughout the shell in the plane of the crack (Fig. 1). Consequently, in the crack problem the plane of the crack would be a plane of symmetry with respect to loading as well as geometry.

2. Differential Equations and the Boundary Conditions

The problem described in Fig. 1 is considered within the confines of linearized shallow shell assumptions and a Reissner type transverse shear theory [7]. Details of the formulation of a general shallow shell leading to a crack problem may be found in [4-6] and [8]. The problem is conveniently formulated in terms of a stress function ϕ, transverse displacement w and two auxiliary functions ψ and Ω. Thus, referring to Appendix A for notation and for definitions of dimensionless and normalized quantities, the basic equilibrium equations of a cylindrical shell may be expressed as follows:

$$\nabla^4\phi - \left(\frac{\lambda_1}{\lambda}\right)^2 \frac{\partial^2 w}{\partial y^2} = 0 \quad , \tag{1}$$

$$\nabla^4 w + \lambda^2\lambda_1^2(1-\kappa\nabla^2) \frac{\partial^2\phi}{\partial y^2} = \lambda^4(1-\kappa\nabla^2) \frac{aq}{h} \quad , \tag{2}$$

$$\kappa\nabla^2\psi - \psi - w = 0 \quad , \tag{3}$$

$$\frac{\kappa(1-\nu)}{2}\ \nabla^2\Omega - \Omega = 0 \quad , \tag{4}$$

where $q(x,y)$ is the transverse shear loading and ψ and Ω are related to rotations β_x and β_y by [5]:

$$\beta_x = \frac{\partial\psi}{\partial x} + \frac{\kappa(1-\nu)}{2}\frac{\partial\Omega}{\partial y} \quad , \quad \beta_y = \frac{\partial\psi}{\partial y} - \frac{\kappa(1-\nu)}{2}\frac{\partial\Omega}{\partial x} \quad . \tag{5}$$

In terms of the stress function ϕ the membrane resultants are defined as

$$N_{xx} = \frac{\partial^2\phi}{\partial y^2} \quad , \quad N_{yy} = \frac{\partial^2\phi}{\partial x^2} \quad , \quad N_{xy} = -\frac{\partial^2\phi}{\partial x\partial y} \quad . \tag{6}$$

Similarly, the moment and the transverse shear resultants are given in terms of the displacement and rotations by

$$M_{xx} = \frac{a}{h\lambda^4}\left(\frac{\partial\beta_x}{\partial x} + \nu\frac{\partial\beta_y}{\partial y}\right) \quad , \quad M_{yy} = \frac{a}{h\lambda^4}\left(\nu\frac{\partial\beta_x}{\partial x} + \frac{\partial\beta_y}{\partial y}\right) \quad ,$$

$$M_{xy} = \frac{a}{h\lambda^4}\frac{1-\nu}{2}\left(\frac{\partial\beta_x}{\partial y} + \frac{\partial\beta_y}{\partial x}\right) \quad , \tag{7}$$

$$V_x = \frac{\partial w}{\partial x} + \beta_x \quad , \quad V_y = \frac{\partial w}{\partial y} + \beta_y \quad . \tag{8}$$

Before stating the boundary conditions one may note that the problem is linear and can be solved by using a superposition technique. Thus, the problem of a relatively thin-walled semi-infinite cylinder without the crack under given external loads may be considered separately from the crack problem in which statically self-equilibrating crack surface tractions are the only external loads. In the former problem the external loads may be the transverse loading q and stress, moment, and transverse shear resultants applied to the end (x_2=0) of the cylinder. In the plane of the crack x_1=0 this solution is assumed to give only normal membrane and bending resultants N_{11} and M_{11} and no

shear stresses (i.e., $N_{12}(0,x_2) = M_{12}(0,x_2) = V_1(0,x_2) = 0$). The equal and opposite of $N_{11}(0,x_2)$ and $M_{11}(0,x_2)$ given by this solution are then used as the crack surface tractions to solve the crack problem. In this study it is assumed that the problem of the semi-infinite cylinder without the crack has been solved and $N_{11}(0,x_2)$ and $M_{11}(0,x_2)$ are known functions.

The part-through crack problem will be solved by using the line-spring model. The integral equations of this problem are obtained by modifying those of the through crack problem to account for the unbroken ligament. The main problem is, therefore, the through crack problem which will first be formulated. Also note that because of symmetry it is sufficient to consider one half ($x>0$) of the shell only. Thus, referring to the insert in Fig. 2 and Appendix A for notation, equations (1)-(8) must be solved under the following boundary conditions:

$$N_{yy}(x,0) = 0,\ N_{xy}(x,0) = 0,\ M_{yy}(x,0) = 0,$$
$$M_{xy}(x,0) = 0,\ V_y(x,0) = 0,\ (0\leq x<\infty)\ , \tag{9}$$

$$N_{xy}(0,y) = 0,\ M_{xy}(0,y) = 0,\ V_x(0,y) = 0,\ (-\infty<y\leq 0)\ , \tag{10}$$

$$N_{xx}(+0,y) = F_1(y)\ ,\ (-d_1<y<-b_1)\ , \tag{11}$$

$$u(0,y) = 0,\ (-\infty<y<-d_1,\ -b_1<y<0)\ , \tag{12}$$

$$M_{xx}(+0,y) = F_2(y)\ ,\ (-d_1<y<-b_1)\ , \tag{13}$$

$$\beta_x(0,y) = 0\ ,\ \ (-\infty<y<-d_1,\ -b_1<y<0)\ , \tag{14}$$

where F_1 and F_2 are related to the uncracked shell solution by

$$F_1(y) = -\frac{N_{11}(0,x_2)}{hE}\ ,\ F_2(y) = -\frac{M_{11}(0,x_2)}{h^2E}\ ,\ (x_2=ay). \tag{15}$$

3. Solution of Differential Equations

In the perturbation problem under consideration q=0 and eliminating ϕ from (1) and (2) we obtain

$$\nabla^4\nabla^4 w + \lambda_1^4(1-\kappa\nabla^2)\frac{\partial^2 w}{\partial y^2} = 0 \quad . \tag{16}$$

Considering the symmetry of the problem, for the shallow cylindrical shell the solution of (16) may be expressed as

$$w(x,y) = \frac{1}{2\pi}\int_{-\infty}^{\infty} f_1(x,\alpha)e^{-iy\alpha}d\alpha + \frac{2}{\pi}\int_{0}^{\infty} f_2(y,\beta)\cos x\beta \, d\beta. \tag{17}$$

Assuming the solution for f_1 and f_2 of the form

$$f_1(x,\alpha) = R(\alpha,m)e^{mx} \ , \ f_2(y,\beta) = S(\beta,n)e^{ny} \ , \tag{18}$$

by substituting from (18) and (17) into (16) the characteristic equations for m and n may be obtained as

$$m^8-4\alpha^2m^6+6\alpha^4m^4-(4\alpha^2+\kappa\lambda_1^4)\alpha^4m^2+\alpha^4[\alpha^4+\lambda_1^4(1+\kappa\alpha^2)] = 0 \ , \tag{19}$$

$$n^8-(4\beta^2+\kappa\lambda_1^4)n^6+[6\beta^4+\lambda_1^4(1+\kappa\beta^2)]n^4-4\beta^6n^2+\beta^8 = 0 \ . \tag{20}$$

The solutions of (19) and (20) have the property

$$m_{j+4} = -m_j \ , \ \mathrm{Re}(m_j) < 0, \ (j=1,\ldots,4) \ , \tag{21}$$

$$n_{j+4} = -n_j \ , \ \mathrm{Re}(n_j) < 0, \ (j=1,\ldots,4) \ . \tag{22}$$

Defining now

$$R(\alpha,m_j) = R_j(\alpha) \ , \ S(\beta,n_j) = S_j(\beta) \ , \ (j=1,\ldots,8) \ , \tag{23}$$

with (17) the solution of (16) satisfying the regularity conditions at $x=\infty$ and $y=-\infty$ may be expressed as

$$f_1(x,\alpha) = \sum_{j=1}^{4} R_j(\alpha)e^{m_j x} , \quad (0<x<\infty) , \tag{24}$$

$$f_2(\beta,y) = \sum_{j=5}^{8} S_j(\beta)e^{n_j y} , \quad (-\infty<y<0) . \tag{25}$$

The functions R_j, $(j=1,\ldots,4)$ and S_j, $(j=5,\ldots,8)$ are as yet unknown.

Similarly, if we let

$$\phi(x,y) = \frac{1}{2\pi}\int_{-\infty}^{\infty} g_1(x,\alpha)e^{-iy\alpha}d\alpha + \frac{2}{\pi}\int_{0}^{\infty} g_2(y,\beta)\cos x\beta \, d\beta, \tag{26}$$

noting that $q=0$ from (1) and (2) the functions g_1 and g_2 may be obtained as follows:

$$g_1(x,\alpha) = -\left(\frac{\lambda_1}{\lambda}\right)^2 \sum_{j=1}^{4} \frac{\alpha^2 R_j(\alpha)}{p_j^2} e^{m_j x} , \quad p_j = m_j^2-\alpha^2, \quad (0<x<\infty) , \tag{27}$$

$$g_2(y,\beta) = \left(\frac{\lambda_1}{\lambda}\right)^2 \sum_{j=5}^{8} \frac{n_j^2 S_j(\beta)}{q_j^2} e^{n_j y} , \quad q_j = n_j^2-\beta^2, \quad (-\infty<y<0). \tag{28}$$

Assuming the solution of (4) of the form

$$\Omega(x,y) = \frac{1}{2\pi}\int_{-\infty}^{\infty} h_1(x,\alpha)e^{-iy\alpha}d\alpha + \frac{2}{\pi}\int_{0}^{\infty} h_2(y,\beta)\sin\beta x \, d\beta, \tag{29}$$

$$h_1(x,\alpha) = A(\alpha,r)e^{rx} , \quad n_2(y,\beta) = B(\beta,s)e^{sy} , \tag{30}$$

it can be shown that

$$h_1(x,\alpha) = A_1(\alpha)e^{r_1 x} , \quad r_1 = -\left[\alpha^2 + \frac{2}{\kappa(1-\nu)}\right]^{\frac{1}{2}}, \quad (0<x<\infty) , \tag{31}$$

$$h_2(y,\beta) = B_2(\beta)e^{s_2 y} , \quad s_2 = +\left[\beta^2 + \frac{2}{\kappa(1-\nu)}\right]^{\frac{1}{2}}, \quad (-\infty<y<0), \tag{32}$$

where $A_1(\alpha)$ and $B_2(\beta)$ are unknown functions.

The transverse shear theory used in this study is equivalent to a tenth order system [4]-[6] (that is, for example, the equilibrium equations of the shell can be expressed in terms of five second order differential equations in five "displacement" quantities u, v, w, β_x and β_y) and the differential equations (1), (2) and (4) provide sufficient number of "integration constants" to account for all boundary conditions. For a unique solution of the problem, it is therefore necessary to use only the particular solution of (3) (after determining the function w). Thus, by assuming

$$\psi(x,y) = \frac{1}{2\pi}\int_{-\infty}^{\infty} \theta_1(x,\alpha)e^{-iy\alpha}d\alpha + \frac{2}{\pi}\int_{0}^{\infty} \theta_2(y,\beta)\cos\beta x\, d\beta, \qquad (33)$$

the functions θ_1 and θ_2 satisfying the regularity conditions at $x=\infty$ and $y=-\infty$ are found to be

$$\theta_1(x,\alpha) = \sum_{j=1}^{4} \frac{R_j(\alpha)}{\kappa p_j - 1} e^{m_j x}, \quad \theta_2(y,\beta) = \sum_{j=5}^{8} \frac{S_j(\beta)}{\kappa q_j - 1} e^{n_j y}. \qquad (34)$$

Ten unknown functions R_j, (j=1,...,4), S_j, (j=5,...,8), A_1 and B_2 which appear in the solution given above are determined by using the eight homogeneous and two mixed boundary conditions (9)-(14).

4. Derivation of Integral Equations

By substituting now from the solution given in the previous section into (5)-(8) and by using the strain displacement relations

$$\varepsilon_{ij} = \frac{1}{2}(u_{i,j}+u_{j,i}+Z_{,i}u_{3,j}+Z_{,j}u_{3,i}), \quad (i,j = 1,2), \qquad (35)$$

all membrane, moment and transverse shear resultants, the rotations, and in-plane displacements can be expressed in terms of the unknown functions R_j, S_j, A_1 and B_2. These expressions are given in Appendix B. In (35) $Z(x_1,x_2)$ gives the distance of the middle surface of the shell from the tangent plane. By substituting from Appendix B into (9) and

by inverting the sine and cosine transforms the homogeneous end conditions may be expressed as follows:

$$\sum_{j=5}^{8} \frac{\beta^3 n_j^2}{q_j^2} S_j(\beta) = \frac{1}{2\pi} \int_{-\infty}^{\infty} \sum_{j=1}^{4} \frac{\alpha^2 m_j^3 R_j(\alpha)}{(m_j^2+\beta^2)p_j^2} d\alpha , \tag{36}$$

$$\sum_{j=5}^{8} \frac{n_j^3}{q_j^2} S_j(\beta) = \frac{i}{2\pi} \int_{-\infty}^{\infty} \sum_{j=1}^{4} \frac{\alpha^3 m_j R_j(\alpha)}{(m_j^2+\beta^2)p_j^2} d\alpha , \tag{37}$$

$$\sum_{j=5}^{8} \frac{\nu\beta^2-n_j^2}{\kappa q_j-1} S_j(\beta) + \frac{\kappa(1-\nu)^2}{2} \beta s_2 B_2(\beta) = -\frac{1}{2\pi} \int_{-\infty}^{\infty} [\sum_{j=1}^{4} \frac{(\nu m_j^2-\alpha^2)m_j R_j(\alpha)}{(\kappa p_j-1)(m_j^2+\beta^2)}$$

$$+ \frac{i\kappa(1-\nu)^2\alpha r_1^2}{2(r_1^2+\beta^2)} A_1(\alpha)]d\alpha , \tag{38}$$

$$\sum_{j=5}^{8} \frac{2\beta n_j}{\kappa q_j-1} S_j(\beta) - \frac{\kappa(1-\nu)}{2} (s_2^2+\beta^2)B_2(\beta) = -\frac{1}{2\pi} \int_{-\infty}^{\infty} [\sum_{j=1}^{4} \frac{2i\alpha\beta m_j R_j(\alpha)}{(\kappa p_j-1)(m_j^2+\beta^2)}$$

$$+ \frac{\kappa(1-\nu)(\alpha^2+r_1^2)\beta}{2(r_1^2+\beta^2)} A_1(\alpha)]d\alpha , \tag{39}$$

$$\sum_{j=5}^{8} \frac{q_j n_j S_j(\beta)}{\kappa q_j-1} - \frac{1-\nu}{2} \beta B_2(\beta) = -\frac{1}{2\pi} \int_{-\infty}^{\infty} [\sum_{j=1}^{4} \frac{\alpha i p_j m_j R_j(\alpha)}{(\kappa p_j-1)(m_j^2+\beta^2)}$$

$$+ \frac{(1-\nu)r_1^2}{2(r_1^2+\beta^2)} A_1(\alpha)]d\alpha . \tag{40}$$

Three more homogeneous conditions may be obtained from (10) which, with (36)-(40) may be used to eliminate eight of the ten unknowns. The mixed boundary conditions (11)-(14) would then give a system of dual integral equations to determine the remaining two unknowns. However,

the problem may also be reduced directly to a system of integral equations by introducing the following new unknown functions:

$$G_1(y) = \frac{\partial}{\partial y} u(+0,y) \ , \ G_2(y) = \frac{\partial}{\partial y} \beta_x(+0,y) \ , \ -\infty<y<0 \ . \tag{41}$$

From (12), (14) and (41) it may be seen that the conditions (12) and (14) are equivalent to

$$G_j(y) = 0, \ -\infty<y<-d_1, \ -b_1<y<0, \ (j=1,2) \ , \tag{42}$$

$$\int_{-d_1}^{-b_1} G_j(y)dy = 0, \ (j=1,2) \ . \tag{43}$$

We may now use (41) in place of (11)-(14) as two additional equations to express all unknowns (R_j, S_j, A_1 and B_2) in terms of G_1 and G_2. Then (11) and (13) with (42) and (43) would provide the information to determine G_1 and G_2. First, by substituting from equations (B11) and (B9) of Appendix B into (41), it may be shown that

$$G_1(y) = -\frac{i}{2\pi}\left(\frac{\lambda_1}{\lambda}\right)^2 \int_{-\infty}^{\infty} \sum_{j=1}^{4} \frac{(1+\nu)\alpha^2-p_j}{p_j^2} R_j(\alpha)\alpha \ e^{-iy\alpha} \ d\alpha \ , \tag{44}$$

$$G_2(y) = -\frac{i}{2\pi}\int_{-\infty}^{\infty} \sum_{j=1}^{4} \frac{\alpha m_j R_j(\alpha)}{\kappa p_j - 1} e^{-iy\alpha} \ d\alpha - \frac{\kappa(1-\nu)}{4\pi}\int_{-\infty}^{\infty} \alpha^2 A_1(\alpha) e^{-iy\alpha} \ d\alpha. \tag{45}$$

Then, by using the relations (B3), (B6) and (B7), after some manipulations it can be shown that equations (10), (44) and (45) are equivalent to

$$\sum_{j=1}^{4} \frac{m_j R_j(\alpha)}{p_j^2} = 0 \ , \tag{46}$$

$$\sum_{j=1}^{4} \frac{m_j R_j(\alpha)}{\kappa p_j - 1} = i\left[\kappa(1-\nu)\alpha + \frac{1}{\alpha}\right] C_2(\alpha) \ , \tag{47}$$

$$\sum_{j=1}^{4} m_j R_j(\alpha) = -\frac{i}{\alpha} C_2(\alpha) \quad , \tag{48}$$

$$\sum_{j=1}^{4} \frac{m_j R_j(\alpha)}{p_j} = -\frac{i}{\alpha} \left(\frac{\lambda_1}{\lambda}\right)^2 C_1(\alpha) \quad , \tag{49}$$

$$A_1(\alpha) = 2\, C_2(\alpha) \quad , \tag{50}$$

where

$$C_j(\alpha) = \int_{-d_1}^{-b_1} G_j(y) e^{i\alpha y}\, dy \quad , \ (j=1,2) \quad . \tag{51}$$

After solving (46)-(49) for R_j and obtaining expressions of the form

$$R_j(\alpha) = \int_{-d_1}^{-b_1} \sum_{k=1}^{2} c_{jk}(\alpha,t) G_k(t)\, dt, \ (j=1,\ldots,4) \quad , \tag{52}$$

from (50), (52) and (36)-(40) one can determine S_j and B_2 and find expressions of the form

$$S_j(\beta) = \int_{-d_1}^{-b_1} \sum_{k=1}^{2} b_{jk}(\beta,t) G_k(t)\, dt \ , \ (j=5,\ldots,8) \quad , \tag{53}$$

$$B_2(\beta) = \int_{-d_1}^{-b_1} \sum_{k=1}^{2} b_{5k}(\beta,t) G_k(t)\, dt \ , \tag{54}$$

where c_{jk} and b_{jk} are quite complicated but known functions.

If we now substitute from (50), (52)-(54), (B1) and (B4) into (11) and (13) we obtain a system of integral equations which, with (43), would determine G_1 and G_2. These equations are of the following form:

$$\lim_{x\to+0}\int_{-d_1}^{-b_1}\sum_{j=1}^{2}\left[\int_{-\infty}^{\infty}V_{kj}(x,\alpha)e^{i(t-y)\alpha}d\alpha+\int_{o}^{\infty}Y_{kj}(y,t,\beta)\cos x\beta d\beta\right]G_j(t)dt$$

$$=F_k(y),\ (k=1,2),\ (-d_1<y<-b_1)\ , \tag{55}$$

where V_{kj} and Y_{kj} are known functions. The kernels defined by the functions V_{kj} and Y_{kj} in (55) exhibit certain singular behavior which may be investigated by examining the asymptotic behavior of these functions for $|\alpha|\to\infty$ and $\beta\to\infty$. The process is relatively straightforward. First one needs to obtain the asymptotic expressions for m_j, n_j, r_1 and s_2 defined respectively by (19), (20), (31) and (32) for large values of $|\alpha|$ and β. These expressions may be obtained as follows:

$$m_j(\alpha)=-|\alpha|\left(1+\frac{p_j}{2\alpha^2}-\frac{{p_j}^2}{8\alpha^4}+\ldots\right),\ (j=1,\ldots,4)\ , \tag{56}$$

$$n_j(\beta)=\beta\left(1+\frac{q_j}{2\beta^2}-\frac{{q_j}^2}{8\beta^4}+\ldots\right),\ (j=5,\ldots,8)\ , \tag{57}$$

$$r_1(\alpha)=-|\alpha|\left(1+\frac{1}{\kappa(1-\nu)\alpha^2}-\ldots\right)\ , \tag{58}$$

$$s_2(\beta)=\beta\left(1+\frac{1}{\kappa(1-\nu)\beta^2}-\ldots\right)\ . \tag{59}$$

Then, by substituting from (56)-(59) into the expressions of V_{kj} and Y_{kj}, the principal parts of the kernels can be separated and can be evaluated in closed form. After somewhat lengthy manipulations the integral equations (55) may be shown to reduce to

$$\int_{-d_1}^{-b_1}\left(\frac{1}{t-y}-\frac{1}{t+y}+\frac{6y}{(t+y)^2}-\frac{4y^2}{(t+y)^3}\right)G_1(t)dt$$

$$+\int_{-d_1}^{-b_1}\sum_{j=1}^{2}k_{1j}(y,t)G_j(t)dt=2\pi F_1(y),\ (-d_1<y<-b_1)\ , \tag{60}$$

$$(1-\nu^2)\int_{-d_1}^{-b_1}\left(\frac{1}{t-y}-\frac{1}{t+y}+\frac{6y}{(t+y)^2}-\frac{4y^2}{(t+y)^3}\right)G_2(t)dt$$

$$+\int_{-d_1}^{-b_1}\sum_{j=1}^{2}k_{2j}(y,t)G_j(t)dt=2\pi\lambda^4\frac{h}{a}F_2(y),\quad(-d_1<y<-b_1),\qquad(61)$$

where k_{ij}, $(i,j=1,2)$ are known bounded functions and the loading functions F_1 and F_2 are given by (15).

It should be pointed out that the dominant kernel found in this study which is given in (60) is identical to that found for the elasticity problem of a plane containing a crack perpendicular to a stress-free boundary [1]. It should also be observed that the dominant kernels associated with the crack opening displacement and the crack surface rotation as given in (60) and (61), respectively, are identical, verifying the result found in [9] for flat plates. These are physically expected results and mean that any peculiar behavior the shell solution may have for b=0 (i.e., for an edge crack) must be identical to that of the corresponding plane elasticity solution.

For b>0 (Fig. 2) the kernels of the integral equations (60) and (61) have simple Cauchy type singularity and consequently the solution is of the following form [10]:

$$G_k(y)=\frac{H_k(y)}{[-(y+d_1)(y+b_1)]^{\frac{1}{2}}},\quad(-d_1<y<-b_1),\ (k=1,2)\quad,\qquad(62)$$

where the unknown functions H_1 and H_2 are bounded in the closed interval $[-d_1, -b_1]$. In this case the problem may easily be solved numerically by using a Gauss-Chebyshev type integration formula [11]. For b=0 the problem is an edge crack problem, the functions G_1 and G_2 are bounded at $y=-b_1=0$, and equations (43) are no longer valid. In this problem too the integral equations may again be solved by using a Gauss-Chebyshev integration formula and by, for example, assuming that $H_k(0) = 0$ (in (62)) in place of conditions (43).

5. Stress Intensity Factors

In the linearized shell theory used in this study the stresses are given in terms of the stress resultants as follows:

$$\sigma^m_{ij}(x_1,x_2) = \frac{1}{h} N_{ij}(x_1,x_2) \ , \ (i,j=1,2) \ , \tag{63}$$

$$\sigma^b_{ij}(x_1,x_2,x_3) = \frac{12x_3}{h^3} M_{ij}(x_1,x_2) \ , \ (i,j=1,2) \ , \tag{64}$$

$$\sigma^s_{3j}(x_1,x_2,x_3) = \frac{3}{2h} V_j(x_1,x_2)[1-(\frac{x_3}{h/2})^2], \ (j=1,2) \ , \tag{65}$$

where the "in-plane" stresses may be combined as

$$\sigma_{ij}(x_1,x_2,x_3) = \sigma^m_{ij}(x_1,x_2) + \sigma^b_{ij}(x_1,x_2,x_3), \ (i,j=1,2) \ . \tag{66}$$

In the symmetric problem under consideration σ_{11} is the only nonzero stress component in the plane of the crack $x_1=0$. Thus, the crack problem is one of Mode I and $k_1(x_2,x_3)$, $(x_2=-b,-d)$ is the only nonzero stress intensity factor which, at the crack tips $x_2=-b$ and $x_2=-d$ may be defined as follows:

$$k_1(-b,x_3) = \lim_{x_2 \to -b} \sqrt{2(x_2+b)}\ \sigma_{11}(0,x_2,x_3) \ , \tag{67}$$

$$k_1(-d,x_3) = \lim_{x_2 \to -d} \sqrt{-2(x_2+d)}\ \sigma_{11}(0,x_2,x_3) \ . \tag{68}$$

From (63), (64) and (66)-(68) it is seen that k_1 would be a linear function in x_3 and, analogous to (66), it would be convenient to express it as

$$k_1(x_2,x_3) = k_m(x_2) + \frac{x_3}{h/2} k_b(x_2), \ x_2 = (-b,-d), \ -\frac{h}{2} < x_3 < \frac{h}{2} \ , \tag{69}$$

where k_m and k_b are associated with the "membrane" and "bending" stresses or N_{11} and M_{11} around the crack tips. Observing now that the left hand sides of the integral equations (60) and (61) give the expressions for N_{xx} and M_{xx} in the outside as well as the inside of the crack on the x_1=0 plane and that only the terms with the dominant kernels would contribute to the singular behavior of N_{xx} and M_{xx}, the stress intensity factors k_m and k_b may easily be evaluated in terms of the unknown functions G_1 and G_2. Thus, by using the properties of singular integrals [10], it may be shown that

$$k_m(-b) = -\frac{E}{2}\sqrt{a}\,H_1(-b_1)\ ,\ k_b(-b) = -\frac{E}{2}\sqrt{a}\,\frac{h/2}{a}\,H_2(-b_1)\ , \qquad (70)$$

$$k_m(-d) = \frac{E}{2}\sqrt{a}\,H_1(-d_1)\ ,\ k_b(-d) = \frac{E}{2}\sqrt{a}\,\frac{h/2}{a}\,H_2(-d_1)\ . \qquad (71)$$

6. The Part-Through Crack

In this paper to solve the part-through crack problem shown in Fig. 1 the line spring model [12] is used. The details of the analysis with regard to the adoption of the model to Reissner plate or shell theory and the comparison of the results with the existing three-dimensional finite element solutions may be found in [13] and [14]. Following [14], the Mode I stress intensity factor along the crack frong is expressed as

$$k_1(y) = \sqrt{h}\,[\sigma(y)g_t(\xi) + m(y)g_b(\xi)],\ \xi = L(y)/h\ , \qquad (72)$$

where the functions σ and m represent the membrane and bending resultants along the net ligament $-d_1<y<-b_1$ and $g_t/\sqrt{\xi}$ and $g_b/\sqrt{\xi}$, (ξ=L/h) are the shape factors obtained from the plane elasticity solution of a strip having a thickness h, containing an edge crack of depth L and subjected to uniform tension or bending away from the crack region. Following are relatively accurate expressions of g_t and g_b:

$$g_t(\xi) = \sqrt{\xi}\,(1.1216 + 6.5200\xi^2 - 12.3877\xi^4 + 89.0554\xi^6$$

$$- 188.6080\xi^8 + 207.3870\xi^{10} - 32.0524\xi^{12}) , \qquad (73)$$

$$g_m(\xi) = \sqrt{\xi}\,(1.1202 - 1.8872\xi + 18.0143\xi^2 - 87.3851\xi^3$$

$$+ 241.9124\xi^4 - 319.9402\xi^5 + 168.0105\xi^6) . \qquad (74)$$

To obtain $\sigma(y)$ and $m(y)$ first the integral equations (60) and (61) are modified as [13], [14]

$$-\gamma_{tt}(y)\int_{-d_1}^{y} G_1(t)dt \mp \gamma_{tb}(y)\int_{-d_1}^{y} G_2(t)dt + \frac{1}{2\pi}\int_{-d_1}^{-b_1}[(\frac{1}{t-y}$$

$$- \frac{1}{t+y} + \frac{6y}{(t+y)^2} - \frac{4y^2}{(t+y)^3})G_1(t) + \sum_{j=1}^{2} k_{1j}(y,t)G_j(t)]dt = F_1(y),$$

$$-d_1 < y < -b_1 , \qquad (75)$$

$$\mp \gamma_{bt}(y)\int_{-d_1}^{y} G_1(t)dt - \gamma_{bb}(y)\int_{-d_1}^{y} G_2(t)dt + \frac{a(1-\nu^2)}{2\pi h\lambda^4}\int_{-d_1}^{-b_1}[(\frac{1}{t-y}$$

$$- \frac{1}{t+y} + \frac{6y}{(t+y)^2} - \frac{4y^2}{(t+y)^3})G_2(t) - \frac{1}{1-\nu^2}\sum_{j=1}^{2} k_{2j}(y,t)G_j(t)]dt = F_2(y) ,$$

$$-d_1 < y < -b_1 \qquad (76)$$

where the functions γ_{ij}, (i,j=t,b) are given in [14] and the upper (i.e., -) and lower (i.e., +) signs are to be used for the outer and the inner surface crack, respectively. After solving (75) and (76) σ and m are then obtained from

$$\sigma(y) = E(\gamma_{tt}u \pm \gamma_{tb}\beta_x) \ , \ m(y) = 6E(\gamma_{bt}u \pm \gamma_{bb}\beta_x) \ , \tag{77}$$

$$u(+0,y) = \int_{-d_1}^{y} G_1(t)dt \ , \ \beta_x(+0,y) = \int_{-d_1}^{y} G_2(t)dt \ , \ -d_1<y<-b_1 \ , \tag{78}$$

where + and - signs are to be used for the external and the internal surface crack, respectively.

7. Numerical Results and Discussion

For the through crack problem the calculated results are shown in Tables 1-4 and Figures 2-11. In the results given in Tables 1-4 it is assumed that in the crack region the shell is subjected to uniform membrane loading or bending, i.e., for the uncracked shell we have

$$N_{11}(0,x_2) = N_o \ , \ M_{11}(0,x_2) = 0 \ , \tag{79}$$

or

$$N_{11}(0,x_2) = 0 \ , \ M_{11}(0,x_2) = M_o \ . \tag{80}$$

Thus the input functions of the integral equations are (see (15))

$$F_1(y) = -N_o/hE, \ F_2(y) = 0 \text{ or } F_1(y) = 0, \ F_2(y) = -M_o/h^2E \ . \tag{81}$$

In the tables the membrane and bending components of the stress intensity factor defined by (69) are normalized as follows:

$$k_{mi}(\alpha_j) = \frac{k_m(\alpha_j)}{\sigma_i\sqrt{a}} \ , \ k_{bi}(\alpha_j) = \frac{k_b(\alpha_j)}{\sigma_i\sqrt{a}} \ , \ \alpha_j = (-d,-b), \ i=(m,b) \ , \tag{82}$$

where α_j refers to the crack tip and for uniform membrane and bending loads the corresponding stresses are given by

$$\sigma_m = N_0/h \ , \ \sigma_b = 6M_0/h^2 \ . \qquad (83)$$

The results are given for various combinations of R/h, a/h and c/a which are the characteristic dimensionless length parameters of the shell (see the insert in Fig. 2). The normalized stress intensity factors given in the tables for c/a = 1 are obtained from the edge crack solution. A partial explanation of the steep rise in the stress intensity factors at x_2=-d as c→a may be found in [9]. For the membrane loading when R→∞ or a→0 the bending component k_{bm} of the stress intensity factor tends to zero and k_{mm} approach the corresponding flat plate solution given in [1]. The tables show the general magnifying effect of the decreasing crack distance c from the boundary and the curvature on the stress intensity factors.

Some results obtained from the uniform external loads (79) and (80) are also shown in Figures 2-6. For a fixed relative crack distance c/a = 1.5 Fig. 2 shows the effect of R/h and a/h on the membrane component of the stress intensity factor. As a/h→0 the results approach the corresponding flat plate values obtained in [1] which are also shown in the figure. Figures 3-6 show the edge crack results. Except for Fig. 5, qualitatively these results are quite similar to those obtained for the infinite shell problem given in [4]. Again it is interesting to observe that as a/h→0 k_{mm} approaches 1.586 given by the plane elasticity solution for an edge crack regardless of the value of R/h. Even though this is the physically expected result, as in the limiting cases given in [9], the surprising aspect of it is its prediction by a shell theory. In an infinitely long cylinder having an axial line crack the curves corresponding to those given in Fig. 3 would tend to k_{mm}=1 as a/h→0. It is therefore tempting to look for a shape factor which, as in flat plates, would be independent of the crack length. However, multiplying the results given in [4] corresponding to those in Fig. 3 for a/h>0 by 1.586, it may be shown that the relative magnification in k_{mm} in the edge crack is considerably greater than that in the infinite cylinder.

It may be seen from Table 3 and Fig. 5 that as in the infinite cylinder case the bending stress intensity factors found for the edge crack too decreases with increasing crack length. In this problem the steep variation of k_{bb} and its convergence to the plane elasticity solution for $a/h \to 0$ may seem to be somewhat unusual but should be physically expected. In fact this behavior is nearly identical to the bending solution of a flat plate with an edge crack given in [9].

In the Gauss-Chebyshev quadrature formulas used in solving the integral equations (60) and (61) the integrals on the left-hand sides are evaluated for certain discrete set of values y_i of normalized variable y. Therefore, one may easily obtain some type of Green's functions for the stress intensity factors by simply taking one element of the column matrices $F_1(y_i)$ and $F_2(y_i)$ non-zero at a time. This was routinely done and the results were printed in solving the problem. By using these results one can calculate the stress intensity factors k_{mm}, k_{bm}, k_{mb}, and k_{bb} for any arbitrary external loads $N_{11}(0,x_2)$ and $M_{11}(0,x_2)$ or $F_1(y)$ and $F_2(y)$. For example, Figures 7-11 show some results for a concentrated wedge loading of a cylinder containing an axial edge crack. Figures 7 and 8 show the membrane and bending components of the Mode I stress intensity factor at the crack tip $x_2=-d$ $k_1(-d,x_3) = k_1(x_3)$ in a cylinder subjected to concentrated wedge forces

$$N_{11}(0,x_2) = -P\delta(x_2) \tag{84}$$

shown in the figure. One may note that, as in wedge-loaded flat plate problems in the shell problem too the stress intensity factor is proportional to $1/\sqrt{a}$ and as $a/h \to 0$ (or $R \to \infty$) again the shell results converge to the plane elasticity values $k_{mm} = 0.58$ (Fig. 7) and $k_{bm} = 0$ (Fig. 8). Figures 9 and 10 show the results analogous to Figures 7 and 8 for membrane wedge forces applied at $x_2 = -a$, i.e., for

$$N_{11}(0,x_2) = -P\delta(x_2+a) \ . \tag{85}$$

The effect of the wedge force location on the membrane component of the stress intensity factor for some selected shell and crack dimensions is shown in Fig. 11. The corresponding stress intensity factor in an infinite plate containing a semi-infinite crack and subjected to wedge forces P at a distance s from the crack tip is known to be

$$k_1 = \frac{\sqrt{2}}{\pi} \frac{P}{h\sqrt{s}} \quad . \tag{86}$$

Thus, since k_1 becomes unbounded as $s \to 0$ in Fig. 11 $P/h\sqrt{s}$ rather than $P/h\sqrt{a}$ is used as the normalizing stress intensity factor. It is seen that as $s \to 0$ the stress intensity factor in the shell approaches the flat plate value given by (86). As in the previous limiting cases discussed in this section in this problem too if the applied loads are very near the crack tips or the length of the (through) crack is very small compared to all other dimensions of the structure (including its thickness), then locally the stress state is indistinguishable from the corresponding plane elasticity solution.

The stress intensity factors obtained for a part-through crack are given in Tables 5-12. Even though the crack profile L(y) can be any smooth function, the results are calculated only for a semi-elliptic inner or outer surface crack in the cylinder. That is, in solving the integral equations (75) and (76) it is assumed that (Fig. 1)

$$L(x_2) = L_0\sqrt{1-\left(\frac{x_2+c}{a}\right)^2} = L_0\sqrt{1-(y+c_1)^2} \ ,$$

$$y = x_2/a, \ c_1 = c/a, \ -d < x_2 < -b, \ -c_1 - 1 < y < -c_1 + 1 \ . \tag{87}$$

The problem is solved by assuming that the applied loads are given by (79) or (80) and hence the input functions in (75) and (76) are given by (81). In both cases only the Mode I stress intensity factor k_1 is nonzero along the crack front. k_t and k_b shown in the tables correspond to the normalized Mode I stress intensity factor obtained for uniform "tension" (79) or for "bending" (80), respectively. k_1 is a

function of x_2 only (Fig. 1) and for the two loading conditions considered is normalized as follows:

$$k_t(\bar{x}) = \frac{k_1(x_2)}{\frac{N_o}{h}\sqrt{h}\, g_t(\xi_o)}, \quad \bar{x} = \frac{x_2+c}{a} = y + c_1, \quad \xi_o = \frac{L_o}{h}, \tag{88}$$

$$k_b(\bar{x}) = \frac{k_1(x_2)}{\frac{6M_o}{h^2}\sqrt{h}\, g_b(\xi_o)}, \quad \bar{x} = \frac{x_2+c}{a} = y + c_1, \quad \xi_o = \frac{L_o}{h}, \tag{89}$$

where L_o is the maximum depth of the crack (Fig. 1) and the shape functions g_t and g_b are given by (73) and (74). One may note that the normalizing stress intensity factors used in (88) and (89) are those obtained from the plane strain solution of an infinite strip having a thickness h and containing an edge crack of depth L_o which is subjected to uniform tension N_o or bending M_o. For the crack depths L_o used in this study the shape factors g_t and g_b are calculated to be

$\xi_o = L_o/h$	0.2	0.4	0.6	0.8
$\sqrt{h/L_o}\, g_t(\xi_o)$	1.3674	2.1119	4.035	11.988
$\sqrt{h/L_o}\, g_b(\xi_o)$	1.0554	1.2610	1.915	4.691

Tables 5-9 show the normalized stress intensity factors k_t and k_b for a certain range of R/h, a/h, c/a and L_o/h which are the dimensionless characteristic length parameters of the problem. It is assumed that the part-through crack may be on the outside or the inside surface of the cylinder. As in the through crack solution, in all calculations the Poisson's ratio ν of the material is assumed to be 0.3. The previous studies varying ν between 0 and 0.5 have shown that its effect on the stress intensity factors is relatively insignificant

(see, for example, [5]). Hence, the results given should be valid for most structural materials. The tables show that the stress intensity factor at the maximum penetration point of a semi-elliptic surface crack appears to be relatively insensitive to the crack distance c from the free end.

Some sample results showing the variation of the stress intensity factor along the crack front are given in Tables 10-12. It is seen that generally at a given crack depth the stress intensity factor at the location nearer to the stress-free boundary is greater than that at the corresponding point which is farther. However, this skewness or non-symmetry in the distribution of the stress intensity factor with respect to the midpoint $\bar{x} = 0$ or $x_2 = -c$ of the crack seems to be surprisingly small.

Acknowledgements. This work was supported by the National Science Foundation under the Grant MEA-8209083 and by NASA-Langley under the Grant NGR 39 007 011. It was completed by the senior author during his stay at the Fraunhofer-Institut fur Werkstoffmechanik in Freiburg, Germany as an Alexander von Humboldt Senior U.S. Scientist Awardee.

References

1. T.S. Cook and F. Erdogan, "Stresses in Bonded Materials with a Crack Perpendicular to the Interface," Int. J. Engng. Sci., Vol. 10, pp. 667-697, 1972.

2. F. Erdogan and K. Arin, "A Half Plane and a Strip with an Arbitrarily Located Crack", Int. J. Fracture Mechanics, Vol. 11, pp. 191-204, 1975.

3. F. Erdogan and G.C. Sih, "On the Crack Extension in Plates under Plane Loading and Transverse Shear", J. Basic Engineering, Trans. ASME, Vol. 85, Series D, pp. 519-526, 1963.

4. S. Krenk, "Influence of Transverse Shear on an Axial Crack in a Cylindrical Shell", Int. J. of Fracture, Vol. 14, pp. 123-143, 1978.

5. F. Delale and F. Erdogan, "Transverse Shear Effect in a Circumferentially Cracked Cylindrical Shell", Quarterly of Applied Mathematics, Vol. 37, pp. 239-258, 1979.

6. F. Delale and F. Erdogan, "Effect of Transverse Shear and Material Orthotropy in a Cracked Spherical Cap", Int. J. Solids Structures, Vol. 15, pp. 907-926, 1979.

7. E. Reissner, "On Bending of Elastic Plates", Quarterly of Applied Mathematics, Vol. 5, pp. 55-68, 1947.

8. O.S. Yahsi and F. Erdogan, "A Cylindrical Shell with an Arbitrarily Oriented Crack", Int. J. Solids Structures, Vol. 19, pp. 955-972, 1983.

9. H. Boduroglu and F. Erdogan, "Internal and Edge Cracks in a Plate of Finite Width under Bending", J. Appl. Mech., Vol. 51, Trans. ASME, 1984 (to appear).

10. N.I. Muskhelishvili, Singular Integral Equations, Noordhoff, Groningen, The Netherlands, 1953.

11. F. Erdogan, "Mixed Boundary Value Problems in Mechanics", Mechanics Today, S. Nemat-Nasser, ed., Vol. 4, pp. 1-86, Pergamon Press, 1978.

12. J.R. Rice and N. Levy, "The Part-Through Surface Crack in an Elastic Plate", J. Appl. Mech., Vol. 39, Trans. ASME, pp. 185-194, 1972.

13. F. Delale and F. Erdogan, "Line-Spring Model for Surface Cracks in a Reissner Plate", Int. J. Engng. Sci., Vol. 19, pp. 1331-1340, 1981.

14. F. Delale and F. Erdogan, "Application of the Line Spring Model to a Cylindrical Shell Containing a Circumferential or an Axial Part-Through Crack", J. Appl. Mech., Vol. 49, Trans. ASME, pp. 97-102, 1982.

APPENDIX A

Dimensionless and Normalized Quantities

$$x = \frac{x_1}{a} , \; y = \frac{x_2}{a} , \; z = \frac{x_3}{a} , \; b_1 = \frac{b}{a} , \; c_1 = \frac{c}{a} , \; d_1 = \frac{d}{a} , \tag{A.1}$$

$$u = u_1/a , \; v = u_2/a , \; w = u_3/a , \tag{A.2}$$

$$\beta_x = \beta_1 , \; \beta_y = \beta_2 , \; \phi(x,y) = \frac{F(x_1,x_2)}{a^2 E h} , \tag{A.3}$$

$$\sigma_{xx} = \sigma_{11}/E , \; \sigma_{yy} = \sigma_{22}/E , \; \sigma_{xy} = \frac{\sigma_{12}}{E} , \; \sigma_{xz} = \frac{\sigma_{13}}{B} , \; \sigma_{yz} = \frac{\sigma_{23}}{B} , \tag{A.4}$$

$$N_{xx} = \frac{N_{11}}{hE} , \; N_{yy} = \frac{N_{22}}{hE} , \; N_{xy} = \frac{N_{12}}{hE} , \; \sigma^m_{ij} = \frac{N_{ij}}{h} , \; (i=1,2) , \tag{A.5}$$

$$M_{xx} = \frac{M_{11}}{h^2 E} , \; M_{yy} = \frac{M_{22}}{h^2 E} , \; M_{xy} = \frac{M_{12}}{h^2 E} , \; \sigma^b_{ij} = \frac{6M_{ij}}{h^2} , \; (i,j=1,2) \tag{A.6}$$

$$V_x = V_1/hB , \; V_y = V_2/hB , \; B = \frac{5E}{12(1+\nu)} \tag{A.7}$$

$$\lambda_1^4 = 12(1-\nu^2)a^4/h^2R^2 , \; \lambda^4 = 12(1-\nu^2)a^2/h^2 , \; \kappa = E/B\lambda^4 , \tag{A.8}$$

For dimensions and notation see Figure 1.

APPENDIX B

Expressions for stress resultants, displacements and rotations.

$$N_{xx}(x,y) = \int_{-\infty}^{\infty} \sum_{1}^{4} \alpha^4 T_{1j} d\alpha + \int_{0}^{\infty} \sum_{5}^{8} n_j^2 L_{1j} \cos\beta x d\beta, \tag{B.1}$$

$$N_{yy}(x,y) = -\int_{-\infty}^{\infty} \sum_{1}^{4} \alpha^2 m_j^2 T_{1j} d\alpha - \int_{0}^{\infty} \sum_{5}^{8} L_{1j} \beta^2 \cos\beta x d\beta , \tag{B.2}$$

$$N_{xy}(x,y) = -i\int_{-\infty}^{\infty} \sum_{1}^{4} \alpha^3 m_j T_{1j} d\alpha + \int_{0}^{\infty} \sum_{5}^{8} \beta n_j L_{1j} \sin\beta x d\beta, \tag{B.3}$$

$$M_{xx}(x,y) = \int_{-\infty}^{\infty} \sum_{1}^{4} (m_j^2 - \nu\alpha^2) T_{2j} d\alpha - \int_{0}^{\infty} \sum_{5}^{8} (\beta^2 - \nu n_j^2) L_{2j} \cos\beta x d\beta$$

$$- \frac{(1-\nu)ia}{h\lambda^4} \int_{-\infty}^{\infty} \alpha\, r_1 T_3 d\alpha + \frac{(1-\alpha)a}{h\lambda^4} \int_{0}^{\infty} \beta\, s_1 L_3 \cos\beta x d\beta , \tag{B.4}$$

$$M_{yy}(x,y) = \int_{-\infty}^{\infty} \sum_{1}^{4} (\nu m_j^2 - \alpha^2) T_{2j} d\alpha - \int_{0}^{\infty} \sum_{5}^{8} (\nu\beta^2 - n_j^2) L_{2j} \cos\beta x d\beta$$

$$+ \frac{(1-\nu)ia}{h\lambda^4} \int_{-\infty}^{\infty} \alpha\, r_1 T_3 d\alpha - \frac{(1-\nu)a}{h\lambda^4} \int_{0}^{\infty} s_1 \beta \cos\beta x d\beta , \tag{B.5}$$

$$M_{xy}(x,y) = -i(1-\nu)\int_{-\infty}^{\infty} \sum_{1}^{4} \alpha\, m_j T_{2j} d\alpha - (1-\nu)\int_{0}^{\infty} \sum_{5}^{8} \beta\, n_j L_{2j} \sin\beta x d\beta$$

$$- \frac{(1-\nu)a}{2h\lambda^4} \int_{-\infty}^{\infty} (\alpha^2 + r_1^2) T_3 d\alpha + \frac{(1-\nu)a}{2h\lambda^4} \int_{0}^{\infty} (s_1^2 + \beta^2) L_3 \sin\beta x d\beta , \tag{B.6}$$

$$V_x(x,y) = \frac{\kappa h\lambda^4}{a} \int_{-\infty}^{\infty} \sum_{1}^{4} p_j m_j T_{2j} d\alpha - \frac{\kappa h\lambda^4}{a} \int_{0}^{\infty} \sum_{5}^{8} \beta q_j L_{2j} \sin\beta x d\beta$$

$$- i\int_{-\infty}^{\infty} \alpha\, T_3 d\alpha + \int_{0}^{\infty} s_1 L_3 \sin\beta x d\beta , \tag{B.7}$$

$$V_y(x,y) = -\frac{i\kappa h\lambda^4}{a}\int_{-\infty}^{\infty}\sum_{1}^{4}\alpha\, p_j T_{2j}\,d\alpha + \frac{\kappa h\lambda^4}{a}\int_{0}^{\infty}\sum_{5}^{8} q_j n_j L_{2j}\cos\beta x\,d\beta$$

$$-\int_{-\infty}^{\infty} r_1 T_3\,d\alpha - \int_{0}^{\infty}\beta\, L_3\cos\beta x\,d\beta\ , \qquad (B.8)$$

$$\beta_x(x,y) = \frac{h\lambda^4}{a}\int_{-\infty}^{\infty}\sum_{1}^{4} m_j T_{2j}\,d\alpha - \frac{h\lambda^4}{a}\int_{0}^{\infty}\sum_{5}^{8}\beta\, L_{2j}\sin\beta x\,d\beta$$

$$-i\int_{-\infty}^{\infty}\alpha\, T_3\,d\alpha + \int_{0}^{\infty} s_1\sin\beta x\,d\beta\ , \qquad (B.9)$$

$$\beta_y(x,y) = -\frac{ih\lambda^4}{a}\int_{-\infty}^{\infty}\sum_{1}^{4}\alpha\, T_{2j}\,d\alpha + \frac{h\lambda^4}{a}\int_{0}^{\infty}\sum_{5}^{8} n_j L_{2j}\cos\beta x\,d\beta$$

$$-\int_{-\infty}^{\infty} r_1 T_3\,d\alpha - \int_{0}^{\infty}\beta\, B_2\cos\beta x\,d\beta\ , \qquad (B.10)$$

$$u(x,y) = \int_{-\infty}^{\infty}\sum_{1}^{4}[(2+\nu)\alpha^2 - m_j{}^2]m_j T_{1j}\,d\alpha + \int_{0}^{\infty}\sum_{5}^{8}(2+\nu)\beta L_{1j}\sin\beta x\,d\beta$$

$$+\left(\frac{\lambda_1}{\lambda}\right)^2 x\, w(x,y)\ , \qquad (B.11)$$

$$v(x,y) = -i\int_{-\infty}^{\infty}\sum_{1}^{4}(\nu\alpha^2+m_j{}^2)\alpha T_{2j}\,d\alpha - \int_{0}^{\infty}\sum_{5}^{8}(\beta^2+\nu n_j{}^2)L_{1j}\frac{\cos\beta x}{n_j}\,d\beta\ , \qquad (B.12)$$

where

$$T_{1j}(x,y,\alpha) = \frac{1}{2\pi}\frac{\lambda_1{}^2}{\lambda^2}\frac{R_j(\alpha)}{p_j{}^2}\,e^{m_j x - i\alpha y}\ ,$$

$$T_{2j}(x,y,\alpha) = \frac{1}{2\pi}\frac{a}{h\lambda^4}\frac{R_j(\alpha)}{\kappa p_j - 1}\,e^{m_j x - i\alpha y}\ ,$$

$$T_3(x,y,\alpha) = \frac{\kappa(1-\nu)}{4\pi} A_1(\alpha) e^{r_1 x - i\alpha y} ,$$

$$L_{1j}(y,\beta) = \frac{2}{\pi} \frac{\lambda_1^2}{\lambda^2} \frac{n_j^2}{q_j^2} S_j(\beta) e^{n_j y} ,$$

$$L_{2j}(y,\beta) = \frac{2}{\pi} \frac{a}{h\lambda^4} \frac{1}{\kappa q_j - 1} S_j(\beta) e^{n_j y} ,$$

$$L_3(y,\beta) = \frac{\kappa(1-\nu)}{\pi} B_2(\beta) e^{s_2 y} .$$

Table 1. Membrane component of the normalized stress intensity factors in a cylindrical shell containing an axial through crack along $-d<x_2<-b$. The end of the cylinder ($x_2=0$) is stress-free and the crack surfaces are subjected to uniform membrane loading ($N_{11}=-N_o$, $M_{11}=0$).

$\frac{R}{h}$	$\frac{c/a}{a/h}$	k_{mm} (-b)				k_{mm} (-d)				
		1.1	1.5	2	10	1	1.1	1.5	2	10
5	1	2.154	1.379	1.221	1.162	2.425	1.417	1.238	1.189	1.159
	2	2.273	1.623	1.538	1.483	3.540	1.664	1.556	1.515	1.483
	3	2.534	2.069	1.906	1.861	4.452	2.073	1.968	1.882	1.861
	10	6.092	4.654	4.494	4.458	9.869	4.871	4.522	4.485	4.458
10	1	2.034	1.334	1.171	1.087	2.098	1.368	1.187	1.125	1.086
	2	2.263	1.438	1.316	1.268	2.874	1.485	1.330	1.297	1.266
	3	2.382	1.654	1.570	1.510	3.635	1.693	1.590	1.541	1.510
	10	3.996	3.699	3.462	3.440	7.677	4.883	3.518	3.455	3.440
25	2	2.102	1.354	1.199	1.119	2.279	1.396	1.241	1.150	1.121
	3	2.242	1.416	1.285	1.240	2.772	1.461	1.297	1.263	1.237
	10	2.946	2.722	2.425	2.421	5.668	2.696	2.522	2.429	2.420
100	1	1.761	1.237	1.110	1.007	1.609	1.239	1.116	1.071	1.007
	2	1.884	1.291	1.142	1.039	1.836	1.306	1.149	1.088	1.037
	3	2.010	1.324	1.165	1.074	2.045	1.359	1.164	1.102	1.073
	10	2.388	1.680	1.595	1.535	3.716	1.713	1.618	1.568	1.535
200	1	1.760	1.228	1.100	1.001	1.588	1.225	1.108	1.000	1.001
	2	1.794	1.257	1.125	1.017	1.723	1.264	1.128	1.078	1.017
	3	1.901	1.298	1.144	1.041	1.856	1.316	1.148	1.090	1.040
	10	2.291	1.577	1.354	1.305	3.035	1.508	1.366	1.340	1.305

Table 2. Bending component of the normalized stress intensity factors in a cylindrical shell containing an axial through crack along $-d<x_2<-b$. The end of the cylinder $x_2=0$ is stress-free and the crack surfaces are subjected to uniform membrane loading ($N_{11}=-N_o$, $M_{11}=0$).

$\frac{R}{h}$	$\frac{c/a}{a/h}$	$k_{bm}(-b)$				$k_{bm}(-d)$				
		1.1	1.5	2	10	1	1.1	1.5	2	10
5	1	0.023	0.016	0.024	0.031	0.060	0.028	0.028	0.029	0.031
	2	0.027	0.048	0.053	0.057	0.094	0.059	0.058	0.057	0.057
	3	0.036	0.071	0.072	0.074	0.118	0.071	0.079	0.074	0.074
	10	0.112	0.120	0.125	0.120	0.169	0.128	0.124	0.125	0.120
10	1	0.014	0.012	0.014	0.020	0.041	0.017	0.016	0.016	0.021
	2	0.025	0.028	0.036	0.039	0.069	0.040	0.041	0.038	0.042
	3	0.027	0.048	0.052	0.056	0.094	0.059	0.057	0.055	0.056
	10	0.083	0.109	0.115	0.113	0.150	0.121	0.115	0.115	0.113
25	2	0.017	0.013	0.016	0.027	0.045	0.018	0.018	0.022	0.025
	3	0.023	0.026	0.030	0.034	0.064	0.032	0.034	0.036	0.036
	10	0.052	0.084	0.084	0.088	0.127	0.094	0.090	0.088	0.088
100	1	0.003	0.004	0.004	0	0.029	0.006	0.005	0.006	0
	2	0.010	0	0	0.010	0.022	0.008	0.005	0.007	0.010
	3	0.013	0.009	0.010	0.016	0.032	0.015	0.013	0.014	0.016
	10	0.026	0.044	0.051	0.052	0.091	0.060	0.055	0.055	0.052
200	1	0.007	0	0.003	0	0.027	0.005	0.007	0.001	0
	2	0.004	0	0	0	0.022	0	0	0	0
	3	0.010	0	0	0.010	0.022	0.009	0.006	0.007	0.010
	10	0.023	0.027	0.034	0.038	0.066	0.039	0.041	0.039	0.038

Table 3. Bending component of the normalized stress intensity factors in a cylindrical shell containing an axial through crack along $-d<x_2<-b$. The end of the cylinder $x_2=0$ is stress-free and the crack surfaces are subjected to uniform bending ($N_{11}=0$, $M_{11}=-M_o$).

$\frac{R}{h}$	$\frac{c/a}{a/h}$	$k_{bb}(-b)$				$k_{bb}(-d)$				
		1.1	1.5	2	10	1	1.1	1.5	2	10
5	1	1.117	0.854	0.791	0.726	1.032	0.771	0.783	0.761	0.727
	2	1.043	0.766	0.715	0.650	0.912	0.764	0.748	0.692	0.651
	3	0.990	0.726	0.675	0.614	0.782	0.721	0.667	0.653	0.613
	10	0.771	0.563	0.524	0.464	0.641	0.555	0.518	0.502	0.468
10	1	1.136	0.862	0.797	0.736	1.030	0.855	0.791	0.768	0.738
	2	1.077	0.786	0.734	0.671	0.970	0.786	0.728	0.709	0.673
	3	1.030	0.746	0.690	0.638	0.883	0.747	0.690	0.678	0.638
	10	0.832	0.616	0.577	0.516	0.687	0.612	0.575	0.555	0.517
25	2	1.109	0.803	0.747	0.690	0.990	0.805	0.743	0.722	0.690
	3	1.076	0.771	0.654	0.664	0.958	0.779	0.718	0.700	0.664
	10	0.909	0.678	0.639	0.584	0.702	0.686	0.625	0.619	0.584
100	1	1.169	0.886	0.816	0.753	0.988	0.871	0.812	0.785	0.753
	2	1.129	0.814	0.756	0.704	0.968	0.817	0.754	0.736	0.704
	3	1.108	0.790	0.739	0.685	0.965	0.798	0.734	0.711	0.687
	10	1.006	0.731	0.690	0.638	0.847	0.746	0.689	0.673	0.638
200	1	1.187	0.869	0.812	0.755	0.995	0.884	0.820	0.783	0.757
	2	1.138	0.819	0.759	0.707	0.953	0.819	0.755	0.737	0.707
	3	1.120	0.785	0.741	0.692	0.953	0.793	0.740	0.719	0.693
	10	1.031	0.749	0.708	0.657	0.919	0.772	0.708	0.689	0.656

Table 4. Membrane component of the normalized stress intensity factors in a cylindrical shell containing an axial through crack along $-d<x_2<-b$. The end of the cylinder $x_2=0$ is stress-free and the crack surfaces are subjected to uniform bending ($N_{11}=0$, $M_{11}=-M_o$).

$\frac{R}{h}$	$\frac{c/a}{a/h}$	$k_{mb}(-b)$				$k_{mb}(-d)$				
		1.1	1.5	2	10	1	1.1	1.5	2	10
5	1	0.135	0.082	0.086	0.101	0.034	0.051	0.072	0.083	0.101
	2	0.228	0.194	0.175	0.167	-0.061	0.119	0.150	0.158	0.167
	3	0.272	0.229	0.180	0.171	-0.316	0.117	0.151	0.171	0.169
	10	-0.511	-0.824	-0.771	-0.840	-3.223	-1.190	-0.847	-0.826	-0.838
10	1	0.092	0.053	0.053	0.072	0.024	0.034	0.043	0.046	0.071
	2	0.195	0.126	0.133	0.133	0.021	0.087	0.126	0.126	0.135
	3	0.237	0.197	0.186	0.174	-0.057	0.131	0.160	0.165	0.175
	10	0.068	-0.166	-0.140	-0.192	-1.886	-0.369	-0.206	-0.160	-0.191
25	2	0.118	0.070	0.073	0.087	0.036	0.046	0.060	0.071	0.087
	3	0.173	0.120	0.126	0.131	0.034	0.080	0.106	0.115	0.130
	10	0.312	0.210	0.164	0.145	-0.769	0.079	0.118	0.155	0.145
100	1	0.036	0.018	0.014	0.013	0.058	0.020	0.014	0.011	0.011
	2	0.056	0.029	0.028	0.039	0.024	0.023	0.023	0.026	0.037
	3	0.085	0.046	0.046	0.060	0.026	0.034	0.039	0.051	0.060
	10	0.254	0.224	0.205	0.196	0.033	0.154	0.185	0.189	0.198
200	1	0.035	0.016	0.004	0.018	0.062	0.020	0.014	0.005	0.015
	2	0.039	0.020	0.016	0.023	0.040	0.017	0.014	0.014	0.021
	3	0.056	0.030	0.029	0.042	0.025	0.026	0.025	0.025	0.041
	10	0.200	0.155	0.158	0.163	0.042	0.114	0.138	0.146	0.164

Table 5. Normalized stress intensity factors in a cylindrical shell with a stress-free end containing an axial semi-elliptic surface crack and subjected to uniform local membrane loading or bending, R/h = 5.

a/h	c/a	L_o = 0.2h		L_o = 0.4h		L_o = 0.6h		L_o = 0.8h	
		$k_t(0)$	$k_b(0)$	$k_t(0)$	$k_b(0)$	$k_t(0)$	$k_b(0)$	$k_t(0)$	$k_b(0)$
Outer Crack, R/h = 5, ν = 0.3									
1	1.1	.843	.833	.561	.507	.292	.189	.090	.008
	1.5	.835	.824	.543	.485	.275	.169	.083	.000
	2	.832	.820	.537	.477	.270	.162	.082	-.001
	10	.827	.815	.529	.468	.266	.157	.081	-.002
2	1.1	.904	.898	.687	.651	.410	.329	.142	.062
	1.5	.900	.894	.678	.639	.400	.315	.137	.056
	2	.898	.891	.673	.633	.395	.309	.135	.054
	10	.894	.887	.664	.623	.387	.299	.133	.051
3	1.1	.930	.926	.757	.730	.497	.429	.191	.116
	1.5	.927	.922	.748	.719	.486	.415	.185	.108
	2	.925	.920	.744	.714	.480	.408	.182	.104
	10	.922	.917	.736	.705	.472	.397	.179	.100
10	1.1	.966	.964	.871	.855	.683	.638	.342	.275
	1.5	.964	.962	.866	.849	.675	.627	.334	.265
	2	.963	.961	.863	.846	.670	.620	.330	.260
	10	.961	.959	.857	.838	.660	.607	.322	.249
Inner Crack, R/h = 5, ν = 0.3									
1	1.1	.831	.820	.539	.480	.274	.168	.085	.001
	1.5	.821	.809	.517	.454	.257	.145	.079	-.006
	2	.816	.803	.508	.443	.250	.137	.077	-.008
	10	.809	.795	.497	.429	.244	.129	.076	-.010
2	1.1	.885	.877	.641	.596	.362	.269	.123	.038
	1.5	.879	.871	.626	.578	.347	.250	.117	.031
	2	.876	.868	.620	.571	.342	.243	.116	.029
	10	.871	.862	.609	.558	.334	.233	.113	.026
3	1.1	.911	.905	.703	.667	.428	.347	.156	.073
	1.5	.907	.901	.691	.654	.415	.330	.151	.066
	2	.905	.898	.685	.646	.408	.321	.147	.062
	10	.901	.894	.676	.635	.399	.310	.145	.058
10	1.1	.960	.957	.846	.828	.627	.577	.286	.215
	1.5	.958	.955	.839	.820	.616	.562	.277	.203
	2	.957	.954	.835	.815	.610	.554	.272	.197
	10	.955	.951	.829	.807	.600	.541	.266	.189

Table 6. Normalized stress intensity factors in a cylindrical shell with a stress-free end containing an axial semi-elliptic surface crack and subjected to uniform local membrane loading or bending, R/h = 10.

$\frac{a}{h}$	$\frac{c}{a}$	$L_o = 0.2h$		$L_o = 0.4h$		$L_o = 0.6h$		$L_o = 0.8h$	
		$k_t(0)$	$k_b(0)$	$k_t(0)$	$k_b(0)$	$k_t(0)$	$k_b(0)$	$k_t(0)$	$k_b(0)$
Outer Crack, R/h = 10, ν = 0.3									
1	1.1	.841	.830	.555	.500	.285	.182	.087	.004
	1.5	.832	.821	.536	.476	.268	.160	.081	-.003
	2	.828	.816	.528	.467	.262	.152	.078	-.005
	10	.823	.811	.521	.458	.257	.146	.077	-.007
2	1.1	.900	.894	.676	.638	.394	.310	.131	.050
	1.5	.896	.890	.664	.624	.380	.291	.124	.041
	2	.894	.887	.660	.619	.376	.286	.122	.039
	10	.891	.884	.653	.610	.369	.278	.121	.037
3	1.1	.928	.923	.746	.718	.475	.405	.172	.095
	1.5	.925	.920	.739	.709	.465	.392	.167	.088
	2	.924	.919	.734	.704	.460	.385	.164	.085
	10	.921	.916	.727	.695	.452	.376	.161	.081
10	1.1	.970	.968	.883	.869	.701	.661	.351	.289
	1.5	.968	.966	.879	.864	.693	.651	.344	.280
	2	.968	.965	.877	.862	.689	.646	.340	.275
	10	.966	.964	.872	.856	.681	.635	.333	.266
Inner Crack, R/h = 10, ν = 0.3									
1	1.1	.834	.823	.542	.484	.275	.169	.084	.000
	1.5	.824	.812	.521	.458	.258	.147	.078	-.006
	2	.818	.806	.511	.446	.250	.137	.076	-.009
	10	.812	.798	.500	.433	.243	.128	.074	-.011
2	1.1	.888	.881	.646	.602	.363	.271	.119	.035
	1.5	.882	.874	.629	.582	.345	.248	.112	.026
	2	.879	.871	.622	.574	.339	.240	.110	.023
	10	.874	.866	.612	.562	.331	.230	.108	.020
3	1.1	.913	.908	.704	.669	.423	.341	.148	.064
	1.5	.909	.903	.692	.654	.408	.322	.141	.056
	2	.907	.901	.687	.648	.403	.315	.139	.053
	10	.903	.897	.678	.637	.394	.304	.136	.050
10	1.1	.963	.961	.853	.837	.635	.588	.287	.218
	1.5	.961	.959	.847	.830	.625	.574	.277	.206
	2	.960	.957	.844	.826	.619	.567	.273	.201
	10	.958	.956	.839	.819	.611	.556	.267	.194

Table 7. Normalized stress intensity factors in a cylindrical shell with a stress-free end containing an axial semi-elliptic surface crack and subjected to uniform local membrane loading or bending, R/h = 25.

a/h	c/a	L_o = 0.2h		L_o = 0.4h		L_o = 0.6h		L_o = 0.8h	
		$k_t(0)$	$k_b(0)$	$k_t(0)$	$k_b(0)$	$k_t(0)$	$k_b(0)$	$k_t(0)$	$k_b(0)$
Outer Crack, R/h = 25, ν = 0.3									
1	1.1	.839	.829	.551	.495	.281	.176	.084	.001
	1.5	.829	.818	.530	.470	.263	.154	.079	-.005
	2	.825	.813	.522	.459	.257	.146	.076	-.008
	10	.820	.808	.514	.449	.251	.139	.075	-.010
2	1.1	.898	.891	.668	.629	.382	.296	.124	.042
	1.5	.892	.885	.653	.610	.365	.273	.116	.032
	2	.890	.883	.647	.603	.359	.265	.113	.029
	10	.887	.880	.641	.596	.354	.259	.112	.027
3	1.1	.925	.920	.735	.705	.455	.381	.157	.078
	1.5	.922	.917	.725	.693	.441	.363	.149	.068
	2	.920	.915	.721	.688	.436	.357	.147	.065
	10	.918	.913	.715	.681	.430	.350	.145	.063
10	1.1	.973	.971	.891	.880	.706	.672	.344	.286
	1.5	.972	.970	.887	.875	.698	.662	.335	.275
	2	.971	.969	.885	.873	.695	.657	.332	.271
	10	.970	.968	.881	.868	.688	.648	.326	.264
Inner Crack, R/h = 25, ν = 0.3									
1	1.1	.835	.824	.543	.486	.275	.168	.083	-.001
	1.5	.826	.814	.523	.461	.258	.148	.078	-.007
	2	.821	.808	.514	.450	.251	.139	.075	-.010
	10	.814	.801	.503	.436	.244	.129	.073	-.012
2	1.1	.892	.885	.652	.611	.367	.276	.119	.034
	1.5	.885	.878	.635	.590	.348	.252	.110	.024
	2	.882	.874	.627	.580	.339	.242	.107	.021
	10	.878	.869	.618	.569	.332	.231	.105	.018
3	1.1	.917	.911	.711	.677	.426	.345	.144	.061
	1.5	.912	.906	.697	.660	.408	.322	.135	.051
	2	.910	.904	.691	.653	.401	.314	.133	.047
	10	.907	.900	.683	.643	.393	.303	.130	.044
10	1.1	.965	.963	.859	.844	.638	.592	.276	.212
	1.5	.964	.962	.853	.837	.628	.579	.270	.201
	2	.963	.961	.850	.834	.622	.573	.266	.195
	10	.961	.959	.846	.828	.615	.563	.261	.189

Table 8. Normalized stress intensity factors in a cylindrical shell with a stress-free end containing an axial semi-elliptic surface crack and subjected to uniform local membrane loading or bending, R/h = 100.

$\frac{a}{h}$	$\frac{c}{a}$	L_o = 0.2h		L_o = 0.4h		L_o = 0.6h		L_o = 0.8h	
		$k_t(0)$	$k_b(0)$	$k_t(0)$	$k_b(0)$	$k_t(0)$	$k_b(0)$	$k_t(0)$	$k_b(0)$
Outer Crack, R/h = 100, ν = 0.3									
1	1.1	.837	.827	.547	.490	.276	.170	.082	-.002
	1.5	.828	.817	.528	.467	.260	.151	.077	-.007
	2	.824	.812	.519	.456	.254	.143	.075	-.009
	10	.818	.805	.509	.444	.247	.134	.073	-.012
2	1.1	.896	.889	.662	.621	.374	.286	.120	.036
	1.5	.890	.883	.646	.602	.356	.263	.112	.027
	2	.887	.880	.639	.594	.349	.254	.109	.023
	10	.884	.877	.632	.586	.342	.245	.106	.020
3	1.1	.923	.918	.726	.695	.442	.366	.149	.068
	1.5	.918	.913	.714	.680	.424	.343	.140	.057
	2	.917	.911	.708	.673	.417	.334	.136	.052
	10	.915	.909	.703	.667	.412	.327	.134	.050
10	1.1	.973	.971	.885	.873	.680	.643	.302	.241
	1.5	.972	.970	.881	.869	.673	.635	.296	.233
	2	.971	.970	.879	.867	.670	.630	.292	.229
	10	.970	.969	.876	.863	.664	.623	.288	.223
Inner Crack, R/h = 100, ν = 0.3									
1	1.1	.836	.825	.543	.485	.273	.166	.081	-.003
	1.5	.827	.815	.525	.463	.258	.148	.077	-.008
	2	.822	.810	.516	.453	.252	.140	.075	-.010
	10	.816	.803	.506	.440	.245	.131	.073	-.012
2	1.1	.894	.887	.656	.615	.368	.278	.117	.033
	1.5	.888	.880	.640	.595	.351	.256	.110	.024
	2	.885	.877	.632	.586	.343	.246	.107	.021
	10	.881	.873	.623	.575	.334	.235	.104	.017
3	1.1	.920	.915	.718	.686	.432	.353	.145	.062
	1.5	.915	.910	.704	.669	.413	.330	.135	.051
	2	.913	.907	.697	.661	.405	.319	.131	.046
	10	.910	.904	.690	.651	.397	.308	.128	.042
10	1.1	.967	.965	.862	.848	.634	.588	.263	.194
	1.5	.966	.964	.857	.841	.624	.575	.254	.183
	2	.965	.963	.854	.838	.619	.569	.251	.179
	10	.964	.962	.850	.833	.612	.560	.246	.173

Table 9. Normalized stress intensity factors in a cylindrical shell with a stress-free end containing an axial semi-elliptic surface crack and subjected to uniform local membrane loading or bending, R/h = 200.

$\frac{a}{h}$	$\frac{c}{a}$	$L_o = 0.2h$		$L_o = 0.4h$		$L_o = 0.6h$		$L_o = 0.8h$	
		$k_t(0)$	$k_b(0)$	$k_t(0)$	$k_b(0)$	$k_t(0)$	$k_b(0)$	$k_t(0)$	$k_b(0)$
Outer Crack, R/h = 200, ν = 0.3									
1	1.1	.837	.827	.546	.489	.275	.169	.075	.094
	1.5	.828	.817	.527	.466	.260	.150	.077	-.008
	2	.824	.811	.518	.455	.253	.141	.075	-.010
	10	.818	.805	.508	.443	.246	.133	.073	-.012
2	1.1	.895	.889	.660	.619	.371	.282	.118	.034
	1.5	.890	.882	.644	.601	.354	.260	.111	.026
	2	.887	.879	.637	.592	.347	.251	.108	.022
	10	.884	.876	.630	.583	.340	.242	.105	.019
3	1.1	.922	.917	.724	.693	.438	.361	.147	.065
	1.5	.918	.913	.711	.677	.421	.339	.138	.054
	2	.916	.910	.705	.670	.414	.330	.134	.050
	10	.914	.908	.700	.663	.407	.322	.131	.047
10	1.1	.972	.970	.880	.868	.667	.628	.286	.223
	1.5	.971	.969	.876	.864	.659	.618	.278	.213
	2	.970	.969	.874	.862	.656	.614	.276	.210
	10	.970	.968	.872	.858	.651	.608	.272	.205
Inner Crack, R/h = 200, ν = 0.3									
1	1.1	.836	.825	.543	.486	.273	.166	.081	-.003
	1.5	.827	.815	.525	.463	.258	.148	.077	-.008
	2	.823	.810	.517	.453	.252	.140	.075	-.010
	10	.817	.804	.506	.440	.245	.131	.073	-.012
2	1.1	.894	.887	.656	.615	.367	.277	.117	.032
	1.5	.888	.881	.641	.596	.351	.256	.110	.024
	2	.885	.878	.634	.588	.344	.247	.107	.021
	10	.882	.873	.625	.577	.335	.236	.104	.017
3	1.1	.920	.915	.719	.687	.432	.353	.144	.062
	1.5	.916	.911	.706	.671	.415	.331	.135	.051
	2	.914	.908	.699	.663	.407	.321	.131	.046
	10	.911	.905	.692	.654	.398	.310	.128	.042
10	1.1	.968	.966	.865	.851	.637	.592	.262	.193
	1.5	.967	.965	.859	.844	.625	.576	.251	.180
	2	.966	.964	.856	.841	.620	.570	.247	.175
	10	.965	.963	.853	.836	.613	.562	.242	.169

Table 10. Distribution of normalized stress intensity factors along the crack front in a cylindrical shell with a stress-free end containing an axial semi-elliptic surface crack and subjected to uniform local membrane loading or bending, $\bar{x} = (x_2+c)/a$, R/h = 10, a/h = 1, c/a = 1.1.

L_o/h	0.2		0.4		0.6		0.8	
$\bar{x}$	k_t	k_b	k_t	k_b	k_t	k_b	k_t	k_b
Outer Crack, R/h = 10, a/h = 1, c/a = 1.1								
.929	.584	.674	.480	.615	.288	.380	.101	.127
.828	.680	.755	.511	.601	.290	.335	.099	.102
.688	.748	.799	.533	.573	.291	.292	.099	.072
.516	.796	.821	.548	.545	.291	.248	.095	.044
.319	.827	.830	.556	.521	.290	.210	.090	.022
.108	.840	.832	.558	.505	.288	.187	.088	.007
0	.841	.830	.555	.500	.285	.182	.087	.004
-.108	.837	.828	.551	.497	.283	.181	.086	.005
-.319	.816	.818	.537	.498	.277	.192	.085	.017
-.516	.777	.800	.516	.505	.267	.217	.086	.034
-.688	.721	.769	.487	.516	.255	.246	.085	.056
-.828	.648	.719	.452	.528	.243	.274	.081	.078
-.929	.553	.639	.414	.533	.232	.306	.078	.097
Inner Crack, R/h = 10, a/h = 1, c/a = 1.1								
.929	.584	.674	.476	.610	.281	.371	.097	.122
.828	.679	.754	.505	.594	.282	.325	.096	.097
.688	.745	.796	.525	.564	.282	.281	.095	.068
.516	.792	.816	.538	.533	.282	.236	.091	.040
.319	.821	.824	.544	.507	.281	.198	.087	.019
.108	.834	.824	.544	.489	.277	.174	.085	.003
0	.834	.823	.542	.484	.275	.169	.084	.000
-.108	.830	.820	.538	.481	.273	.168	.083	.002
-.319	.809	.811	.524	.483	.266	.179	.082	.043
-.516	.772	.794	.504	.491	.257	.204	.082	.029
-.688	.717	.765	.477	.504	.246	.234	.081	.051
-.828	.646	.717	.444	.519	.235	.264	.077	.073
-.929	.551	.638	.408	.526	.225	.297	.075	.093

Table 11. Distribution of normalized stress intensity factors along the crack front in a cylindrical shell with a stress-free end containing an axial semi-elliptic surface crack and subjected to uniform local membrane loading or bending, $\bar{x} = (x_2+c)/a$.

L_o/h	0.2		0.4		0.6		0.8	
$\bar{x}$	k_t	k_b	k_t	k_b	k_t	k_b	k_t	k_b
Outer Crack, R/h = 10, a/h = 3, c/a = 1.1								
.929	.549	.639	.456	.604	.330	.457	.151	.203
.828	.671	.749	.541	.654	.372	.458	.161	.109
.688	.768	.824	.616	.683	.411	.454	.170	.169
.516	.845	.876	.678	.703	.444	.440	.174	.142
.319	.898	.908	.723	.715	.460	.421	.173	.117
.108	.925	.922	.745	.719	.475	.408	.172	.098
0	.928	.923	.746	.718	.475	.405	.172	.095
-.108	.924	.921	.742	.716	.472	.404	.171	.096
-.319	.894	.903	.713	.704	.455	.408	.169	.111
-.516	.838	.868	.662	.683	.425	.416	.165	.130
-.688	.759	.814	.593	.654	.384	.419	.156	.149
-.828	.659	.736	.512	.617	.337	.412	.141	.163
-.929	.528	.625	.423	.563	.289	.403	.126	.171
Inner Crack, R/h = 10, a/h = 3, c/a = 1.1								
.929	.554	.645	.467	.616	.332	.459	.144	.195
.828	.675	.753	.546	.659	.366	.450	.150	.176
.688	.768	.824	.610	.675	.392	.430	.154	.148
.516	.840	.870	.659	.680	.411	.400	.154	.116
.319	.888	.896	.691	.678	.422	.368	.150	.089
.108	.911	.907	.704	.672	.425	.346	.148	.068
0	.913	.908	.704	.669	.423	.341	.148	.064
-.108	.909	.905	.699	.666	.419	.340	.146	.065
-.319	.881	.889	.675	.659	.406	.347	.143	.080
-.516	.829	.858	.633	.648	.384	.365	.141	.100
-.688	.754	.808	.574	.631	.354	.380	.135	.122
-.828	.658	.734	.503	.606	.318	.387	.124	.142
-.929	.537	.626	.421	.560	.278	.388	.114	.155

Table 12. Distribution of normalized stress intensity factors along the crack front in a cylindrical shell with a stress-free end containing an axial semi-elliptic surface crack and subjected to uniform local membrane loading or bending, R/h = 25, a/h = 1, c/a = 1.1, $\bar{x} = (x_2+c)/a$.

L_o/h	0.2		0.4		0.6		0.8	
	k_t	k_b	k_t	k_b	k_t	k_b	k_t	k_b
$\bar{x}$	Outer Crack, R/h = 25, a/h = 1, c/a = 1.1							
.929	.584	.675	.479	.614	.285	.377	.099	.125
.828	.680	.755	.509	.599	.286	.331	.097	.099
.688	.747	.798	.531	.570	.287	.287	.096	.070
.516	.795	.820	.545	.541	.287	.242	.092	.041
.319	.825	.829	.553	.517	.286	.204	.087	.019
.108	.839	.830	.553	.500	.283	.181	.085	.004
0	.839	.829	.551	.495	.281	.176	.084	.001
-.108	.835	.826	.547	.492	.278	.176	.084	.003
-.319	.814	.816	.534	.494	.272	.187	.083	.014
-.516	.776	.799	.513	.502	.263	.212	.083	.032
-.688	.721	.769	.485	.513	.252	.242	.084	.054
-.828	.648	.719	.450	.526	.240	.271	.083	.076
-.929	.553	.639	.413	.532	.230	.304	.079	.096
	Inner Crack, R/h = 25, a/h = 1, c/a = 1.1							
.929	.583	.674	.475	.609	.280	.369	.096	.121
.828	.678	.753	.504	.593	.281	.324	.094	.096
.688	.745	.796	.525	.563	.281	.280	.094	.066
.516	.792	.817	.539	.534	.281	.235	.090	.039
.319	.822	.825	.545	.508	.280	.196	.086	.017
.108	.835	.826	.546	.491	.277	.173	.084	.002
0	.835	.824	.543	.486	.275	.168	.083	-.001
-.108	.831	.822	.539	.483	.272	.168	.082	.000
-.319	.811	.812	.526	.485	.266	.179	.081	.012
-.516	.773	.795	.506	.494	.258	.205	.082	.029
-.688	.719	.766	.479	.507	.247	.235	.081	.051
-.828	.646	.718	.446	.521	.235	.265	.077	.074
-.929	.552	.638	.410	.528	.226	.298	.075	.093

Figures

Fig. 1 Geometry of the semi-infinite cylinder with a part-through crack.

Fig. 2 Variation of the membrane component of the normalized stress intensity factors in a semi-infinite cylinder containing a through crack and subjected to uniform membrane loading $N_{11}=N_o$ in the crack region. $k_{mm}(-b)=1.204$ and $k_{mm}(-d)=1.097$ shown in the figure are the stress intensity factors in a semi-infinite plate with the same crack size, relative crack location and loading as the shell.

Fig. 3 Membrane component of the normalized stress intensity factor in a semi-infinite cylinder containing an axial edge crack and subjected to uniform membrane loading $N_{11}=N_o$ in the crack region.

Fig. 4 Bending component of the normalized stress intensity factor in a semi-infinite cylinder containing an axial edge crack and subjected to uniform membrane loading $N_{11}=N_o$ in the crack region.

Fig. 5 Bending component of the normalized stress intensity factor in a semi-infinite cylinder with an axial edge crack which is subjected to uniform bending $M_{11}=M_o$ in the crack region.

Fig. 6 Membrane component of the normalized stress intensity factor in a semi-infinite cylinder having an axial edge crack and subjected to uniform bending $M_{11}=M_o$ in the crack region.

Fig. 7 Membrane component of the normalized stress intensity factor in a semi-infinite cylinder containing an axial edge crack and subjected to concentrated membrane wedge forces P at the circular boundary.

Fig. 8 Bending component of the normalized stress intensity factor in a semi-infinite cylinder having an axial edge crack and subjected to concentrated membrane wedge forces P at the circular boundary.

Fig. 9 Membrane component of the normalized stress intensity factor in a semi-infinite cylinder having an axial edge crack and subjected to membrane wedge forces P at the midpoint of the crack.

Fig. 10 Bending component of the normalized stress intensity factor in a semi-infinite cylinder having an axial edge crack and subjected to membrane wedge forces P at the midpoint of the crack.

Fig. 11 Effect of the location of concentrated membrane wedge forces on the membrane component of the normalized stress intensity factor in a semi-infinite cylinder containing an axial edge crack.

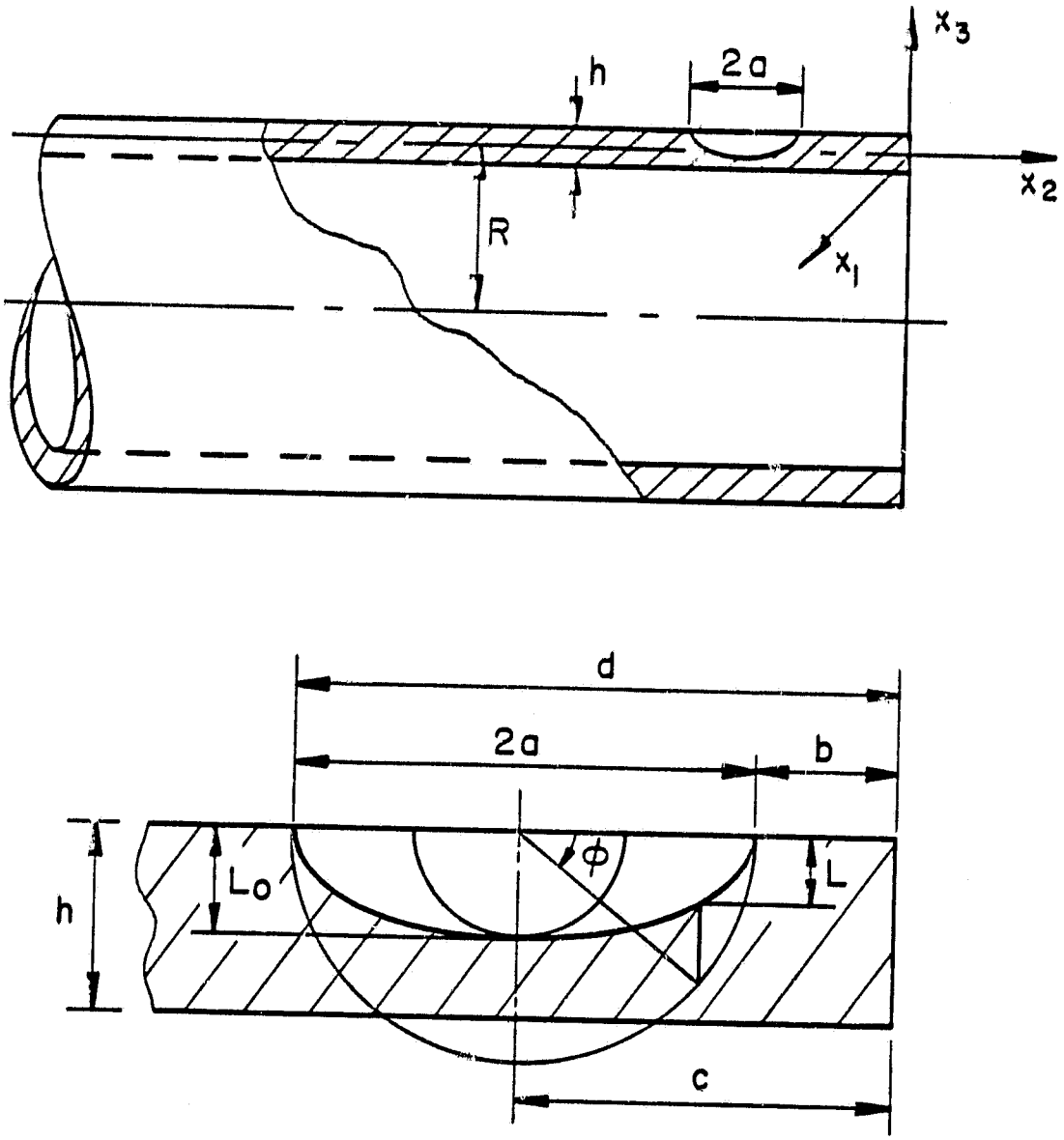

Fig. 1 Geometry of the semi-infinite cylinder with a part-through crack.

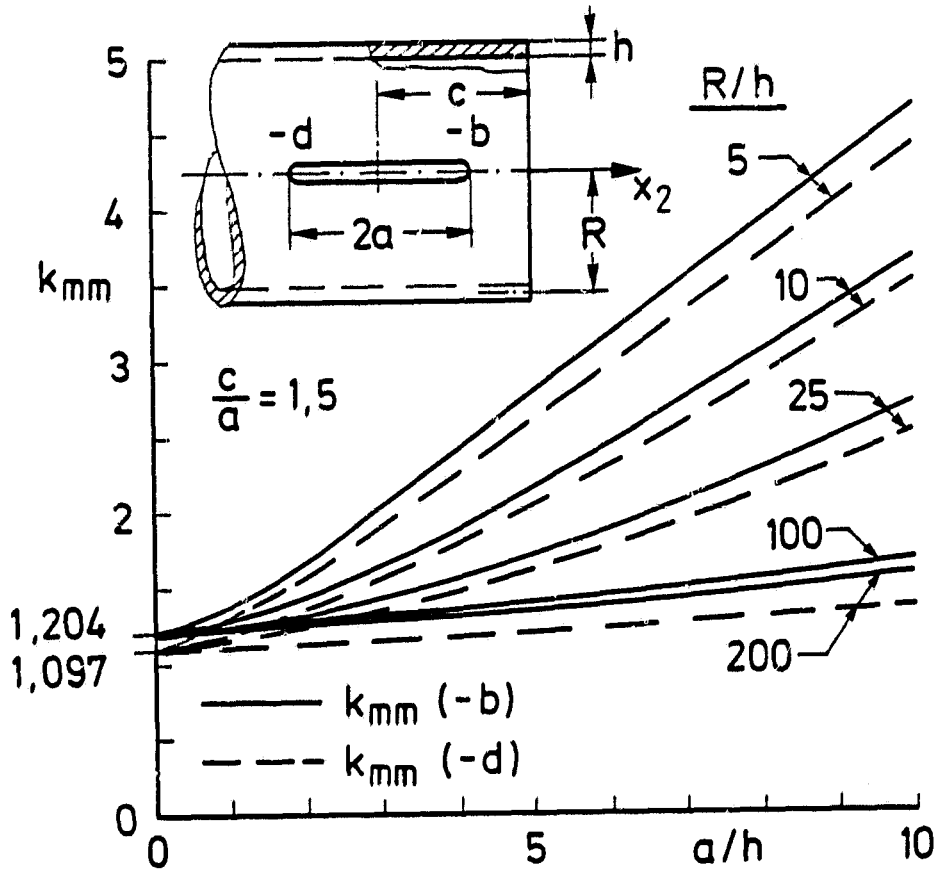

Fig. 2 Variation of the membrane component of the normalized stress intensity factors in a semi-infinite cylinder containing a through crack and subjected to uniform membrane loading $N_{11}=N_o$ in the crack region. $k_{mm}(-b)=1.204$ and $k_{mm}(-d)=1.097$ shown in the figure are the stress intensity factors in a semi-infinite plate with the same crack size, relative crack location and loading as the shell.

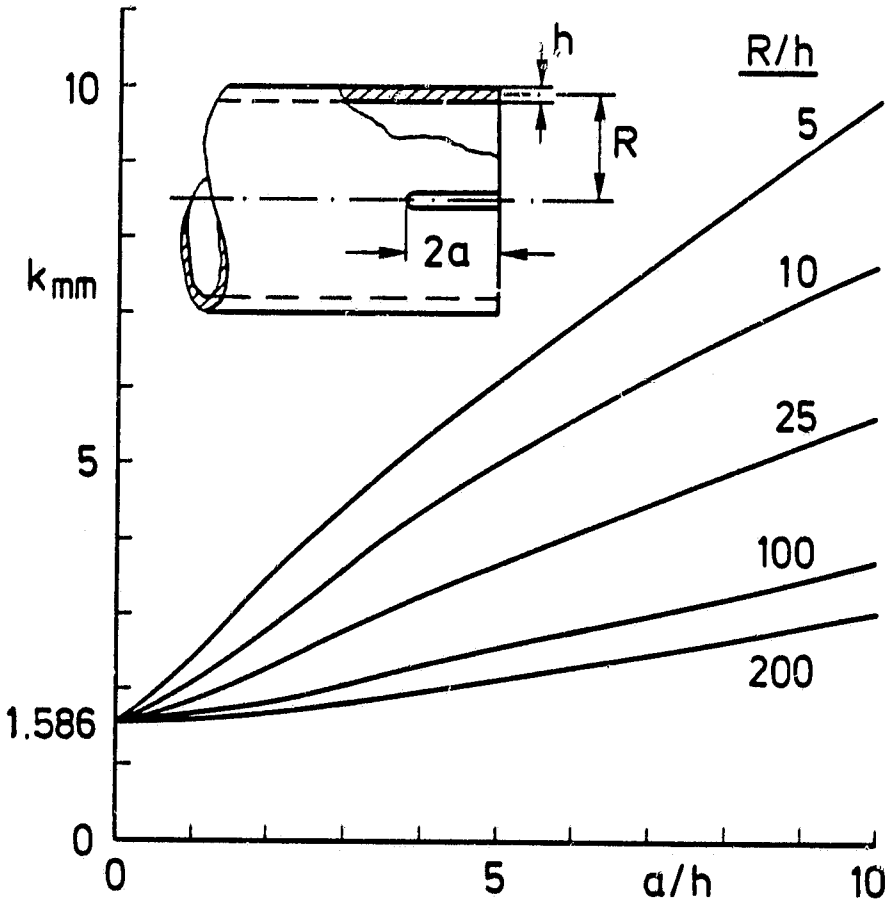

Fig. 3 Membrane component of the normalized stress intensity factor in a semi-infinite cylinder containing an axial edge crack and subjected to uniform membrane loading $N_{11}=N_o$ in the crack region.

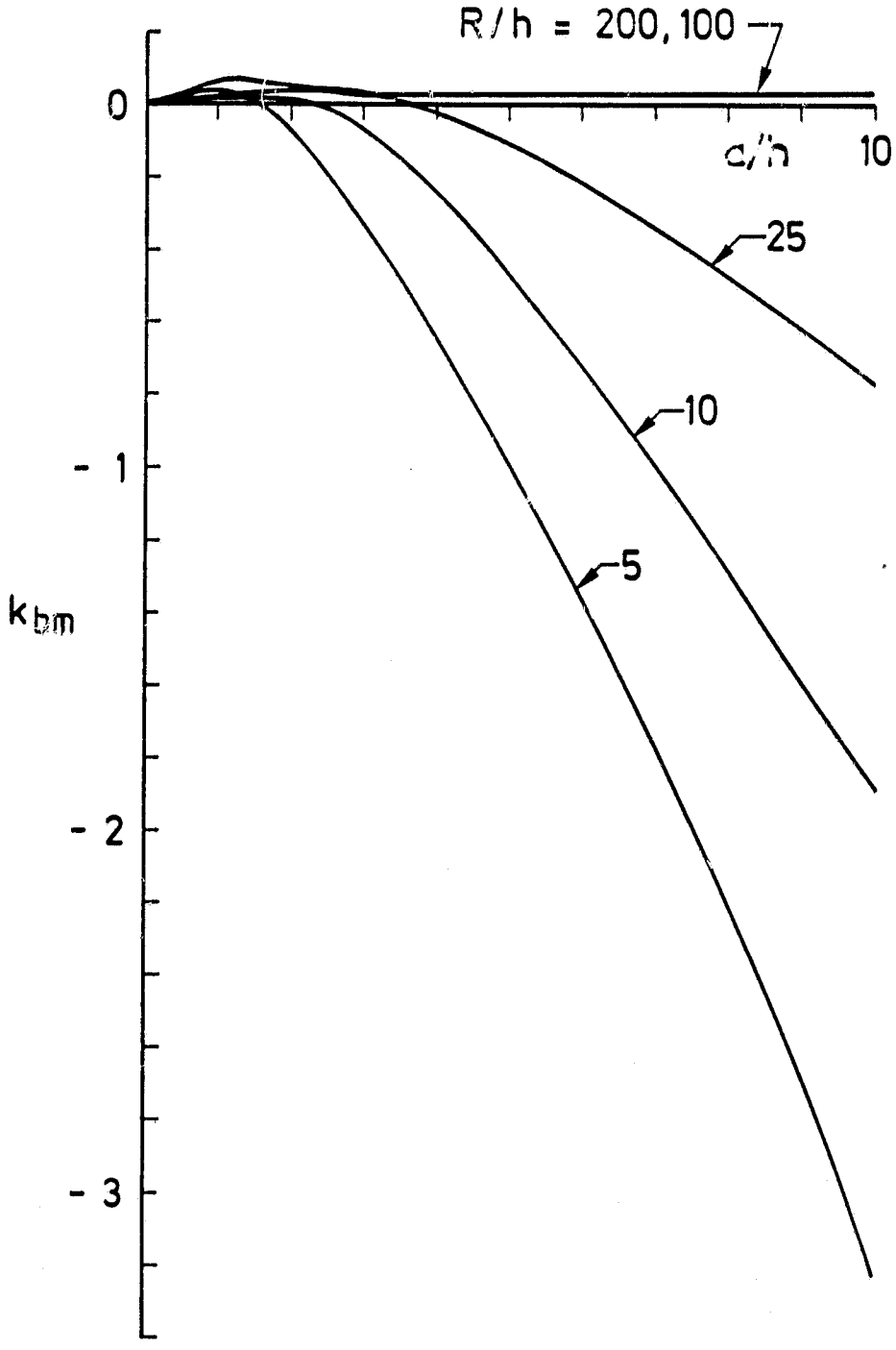

Fig. 4 Bending component of the normalized stress intensity factor in a semi-infinite cylinder containing an axial edge crack and subjected to uniform membrane loading $N_{11}=N_o$ in the crack region.

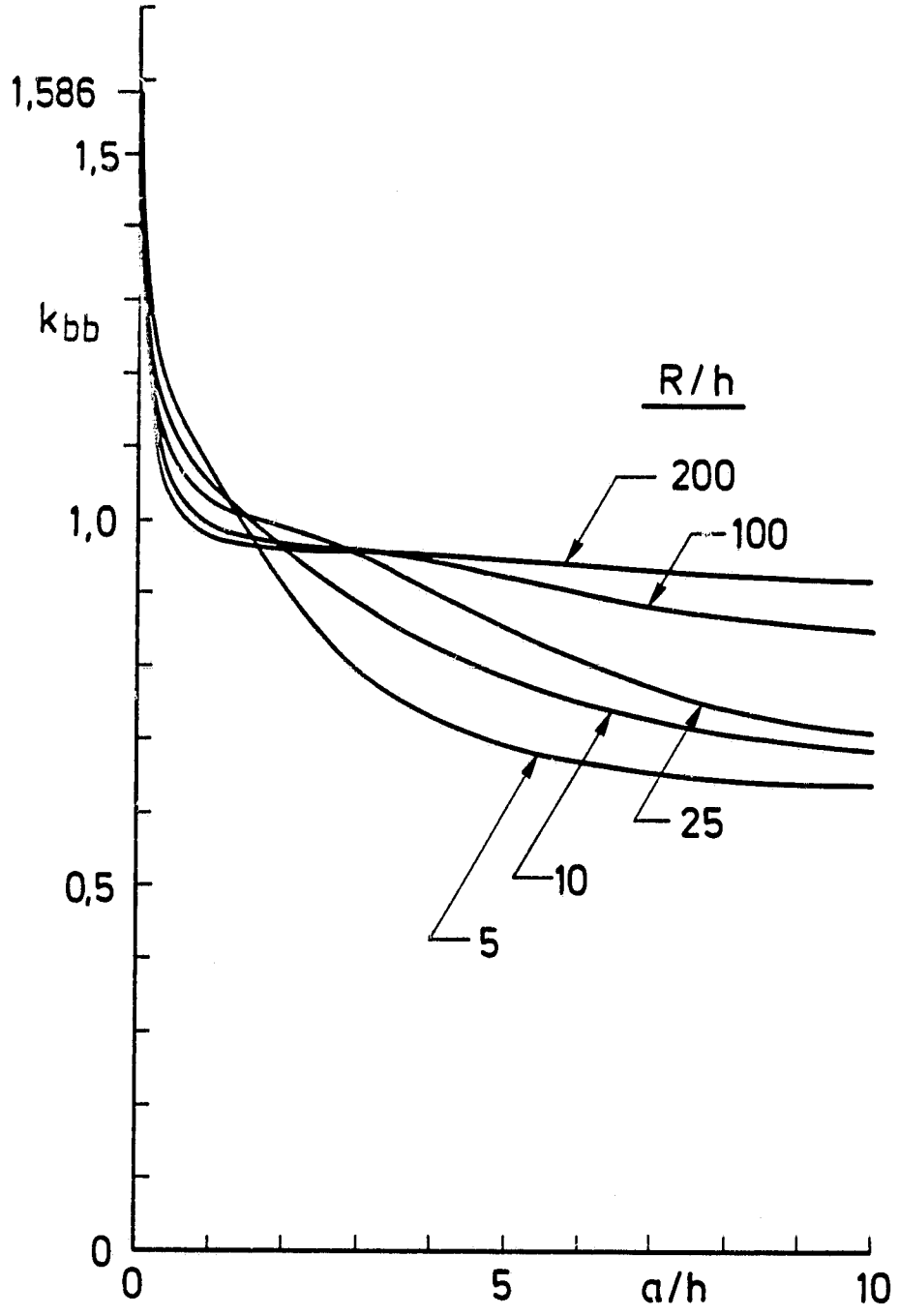

Fig. 5 Bending component of the normalized stress intensity factor in a semi-infinite cylinder with an axial edge crack which is subjected to uniform bending $M_{11}=M_o$ in the crack region.

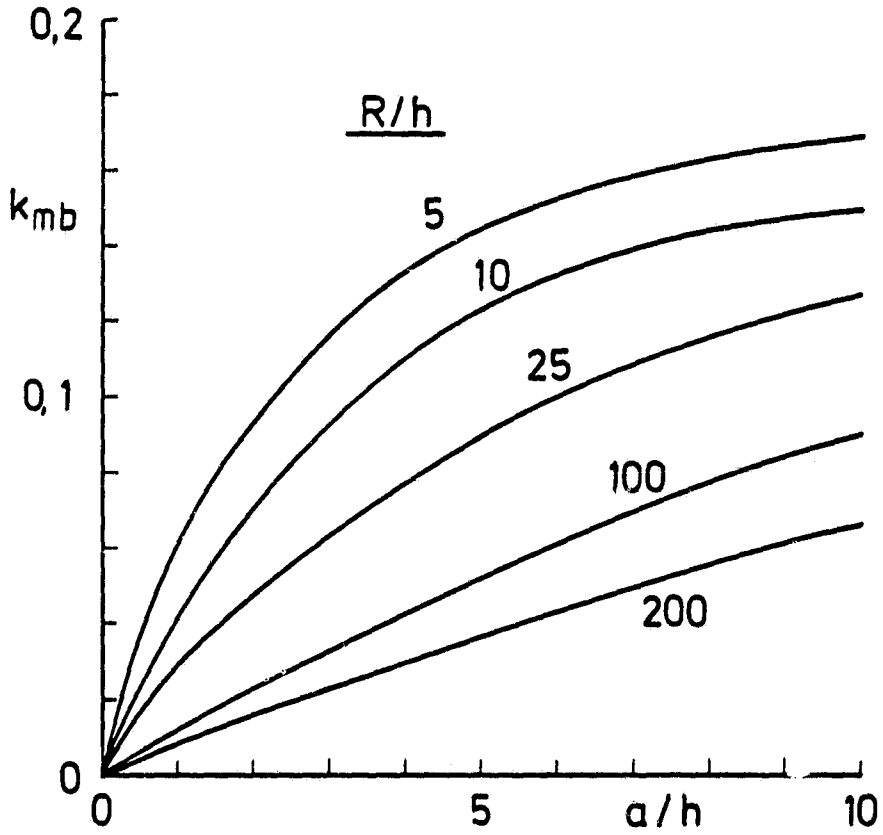

Fig. 6 Membrane component of the normalized stress intensity factor in a semi-infinite cylinder having an axial edge crack and subjected to uniform bending $M_{11}=M_o$ in the crack region.

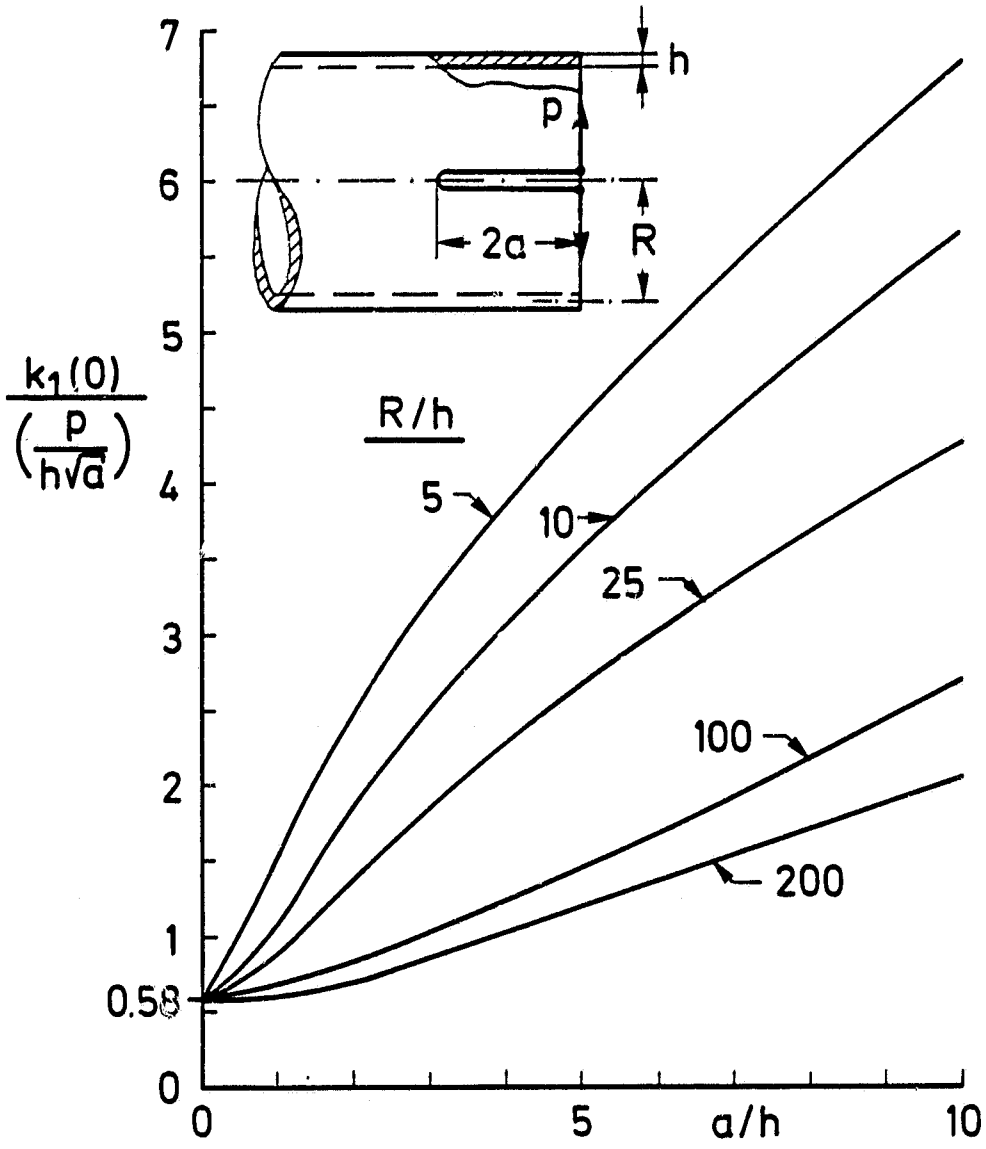

Fig. 7 Membrane component of the normalized stress intensity factor in a semi-infinite cylinder containing an axial edge crack and subjected to concentrated membrane wedge forces P at the circular boundary.

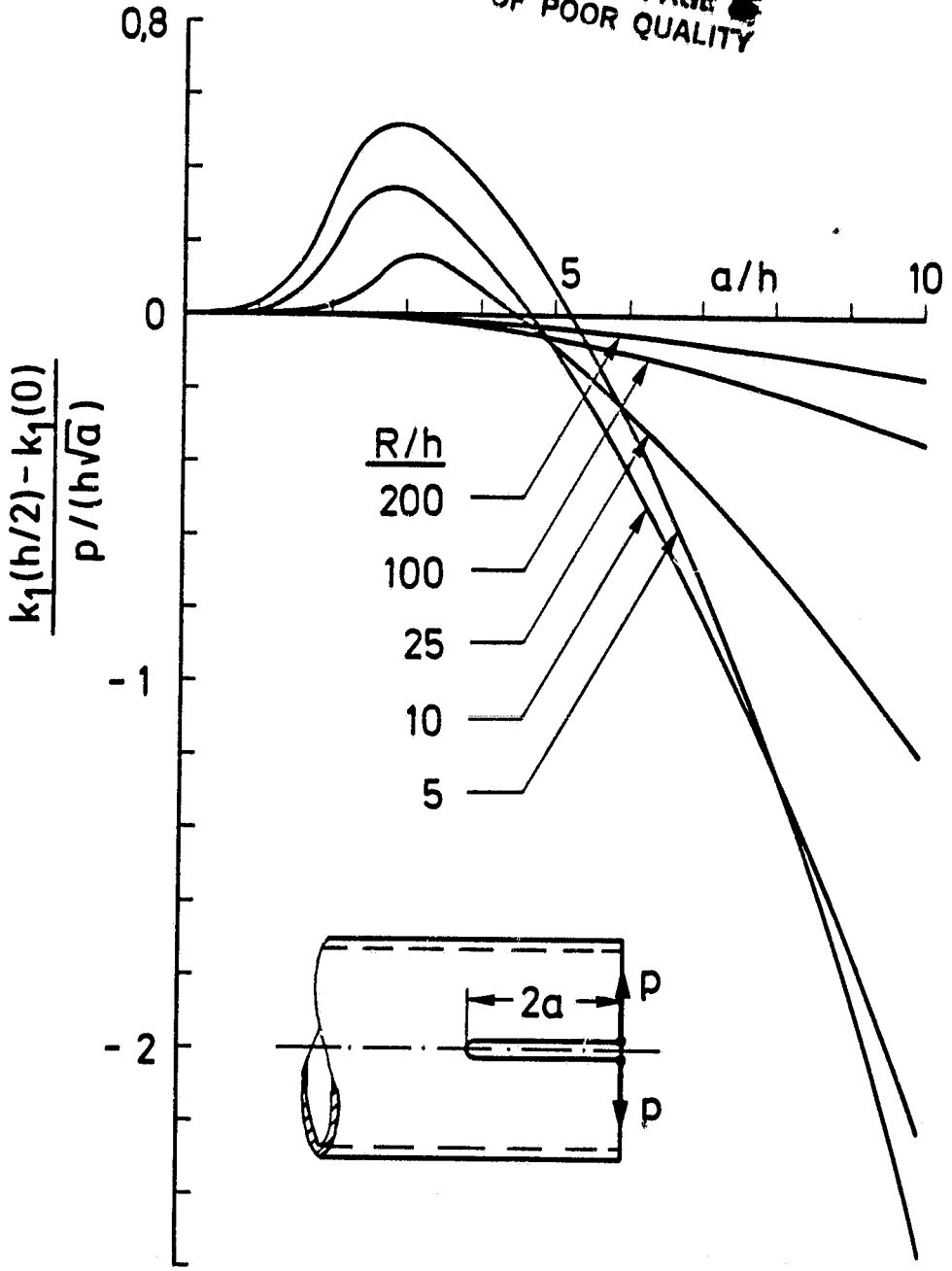

Fig. 8 Bending component of the normalized stress intensity factor in a semi-infinite cylinder having an axial edge crack and subjected to concentrated membrane wedge forces P at the circular boundary.

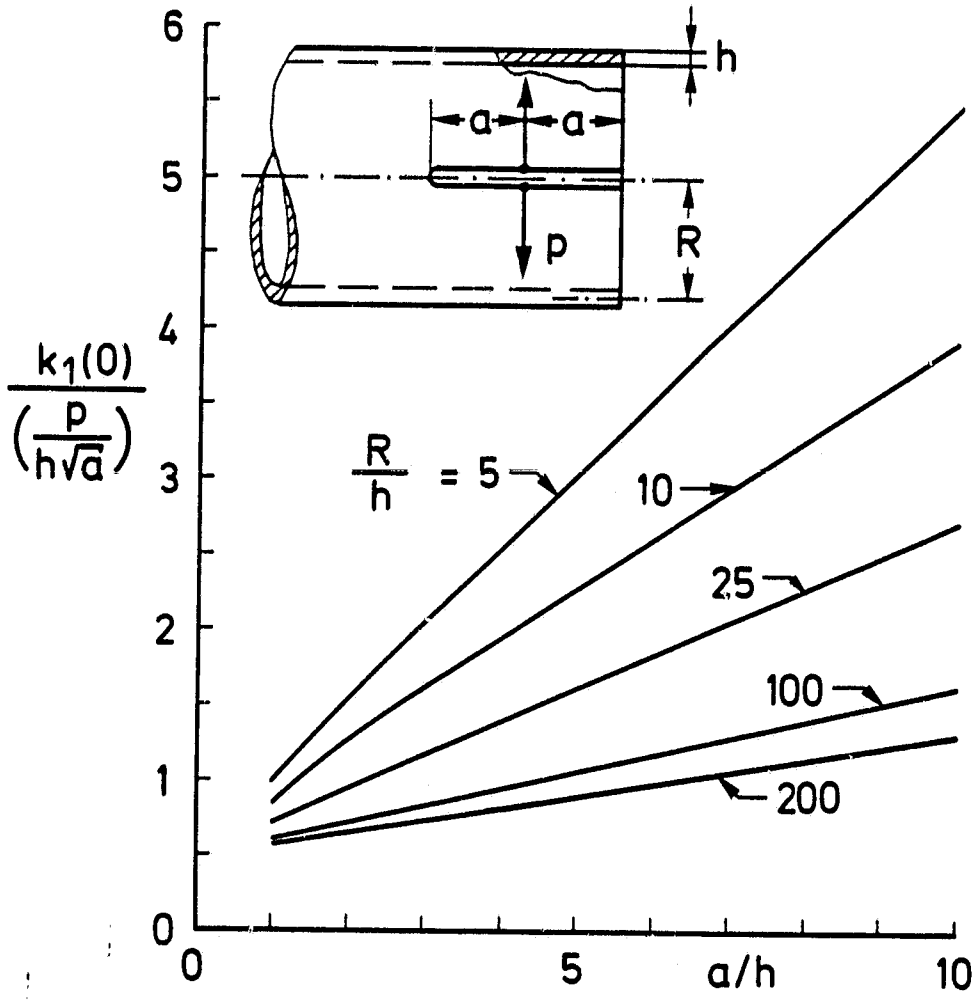

Fig. 9 Membrane component of the normalized stress intensity factor in a semi-infinite cylinder having an axial edge crack and subjected to membrane wedge forces P atthe midpoint of the crack.

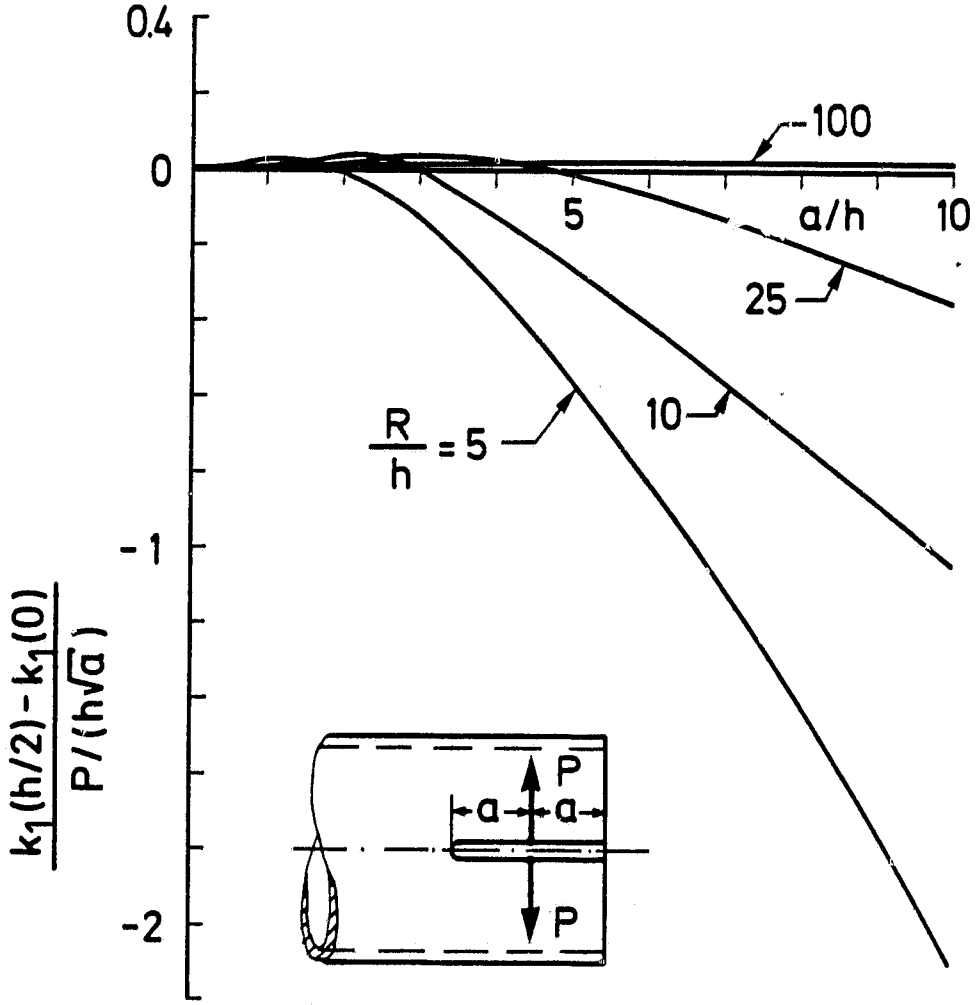

Fig. 10 Bending component of the normalized stress intensity factor in a semi-infinite cylinder having an axial edge crack and subjected to membrane wedge forces P at the midpoint of the crack.

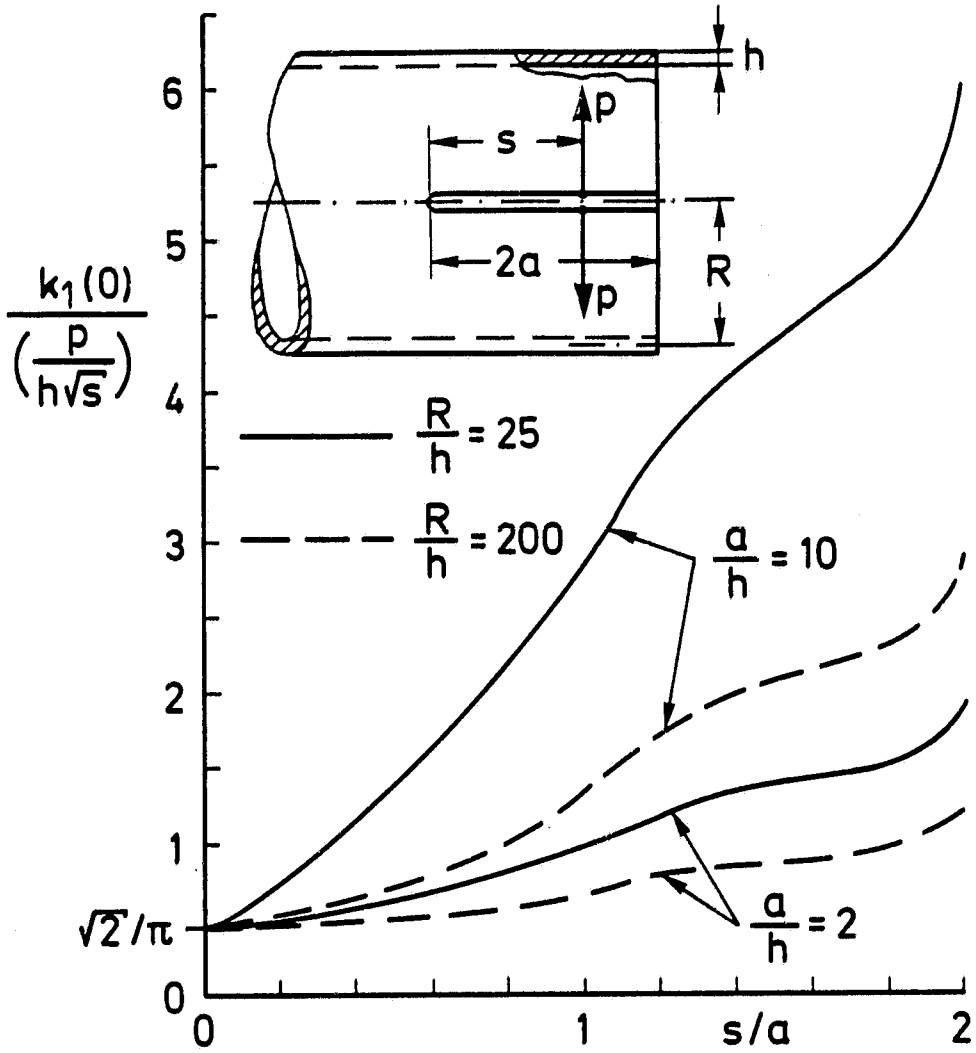

Fig. 11 Effect of the location of concentrated membrane wedge forces on the membrane component of the normalized stress intensity factor in a semi-infinite cylinder containing an axial edge crack.